Most Probable Densest Subgraphs

Arkaprava Saha
NTU, Singapore
saha0003@e.ntu.edu.sg

Xiangyu Ke
ZJU, China
xiangyu.ke@zju.edu.cn

Arijit Khan
AAU, Denmark
arijitk@cs.aau.dk

Cheng Long
NTU, Singapore
c.long@ntu.edu.sg

***Abstract*—Computing the densest subgraph is a primitive graph operation with critical applications in detecting communities, events, and anomalies in biological, social, Web, and financial networks. In this paper, we study the novel problem of Most Probable Densest Subgraph (MPDS) discovery in uncertain graphs: Find the node set that is the *most likely* to induce a densest subgraph in an uncertain graph. We further extend our problem by considering various notions of density, e.g., clique and pattern densities, studying the top-k MPDSs, and finding the node set with the largest containment probability within densest subgraphs. We show that it is #P-hard to compute the probability of a node set inducing a densest subgraph. We then devise sampling-based efficient algorithms, with end-to-end accuracy guarantees, to compute the MPDS. Our thorough experimental results and real-world case studies on brain and social networks validate the effectiveness, efficiency, and usefulness of our solution.**

***Index Terms*—uncertain graphs, densest subgraphs**

I. Introduction

The discovery of dense subgraphs has attracted extensive attention in the data management community [1], [2], [3], [4], [5]. They may correspond to communities [6], filter bubbles and echo chambers [7], [8] in social networks, brain regions responding to stimuli [9] or related to diseases [10], and commercial value motifs in financial domains [11]. They also have wide applications in graph compression and visualization [12], [13], [14], indexing for reachability and distance queries [15], [16], and social piggybacking [17]. Densest subgraphs usually maximize some notion of density in a given graph, e.g., the *edge density* [1], defined as the ratio of the number of induced edges to the number of nodes in a subgraph. Although there are an exponential number of subgraphs, a densest subgraph can be found both exactly and approximately in polynomial time [1], [2]. There also exist many other density metrics [18], such as the edge ratio, edge surplus, triangle, clique, and pattern density, etc. [19], [20], [21], [5].

Uncertainty is intrinsic in large graphs due to errors in measurements [22], edge imputation using inference and prediction models [23], [24], and explicit manipulation including privacy reasons [25]. An uncertain graph, where every edge is associated with a probability of existence, is an expressive data model that has prompted a great deal of research [26], [27], [28]. Recently, researchers have extended several classic network problems to uncertain graphs, e.g., nearest neighbors [29], shortest paths and centrality [30], cliques [31], [32], [33], [34], core and truss decomposition [35], [36], clustering [37], [38], [39], reliable subgraphs [40], and motif counting [41]. Surprisingly, except for maximum *expected edge density* [42], the study of densest subgraph discovery on uncertain graphs is still absent. The expected edge density of an uncertain graph is defined as the expectation of the edge density value of a possible world (i.e., a deterministic graph) of the uncertain graph, chosen at random [42]. However, a subgraph of the uncertain graph having the maximum expected edge density may induce densest subgraphs *only in a few* (even zero) possible worlds of that uncertain graph. Such a subgraph can be large with many low-probability edges, or having nodes that are loosely connected (see Example 1). This defeats the purpose of finding a densest subgraph. Instead, many applications would require a densest subgraph with a high precision, such as being the densest with a high probability. Specifically, given an uncertain graph $\mathcal{G}$, *our goal is to find the node set that is the most likely to induce a densest subgraph in* $\mathcal{G}$, i.e., maximize the sum of the probabilities of those possible worlds of $\mathcal{G}$ in which this node set induces a densest subgraph. We refer to the uncertain subgraph induced by this node set as the *most probable densest subgraph* (MPDS). To the best of our knowledge, computing the MPDS is a novel problem. We demonstrate real-world applications and case studies of our problem on uncertain brain (§ VI-D) and social (§ VI-C) networks, where our proposed MPDS distinguishes healthy brains from those with autism and identifies meaningful communities in a social network.

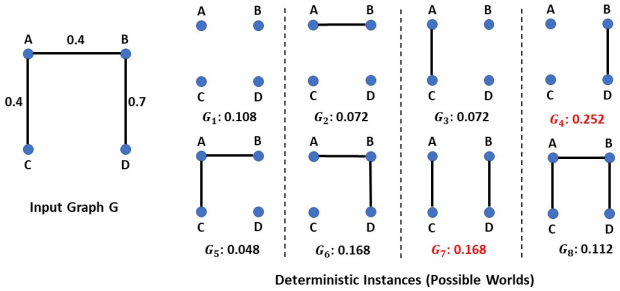

Fig. 1: Possible worlds of an uncertain graph and their probabilities

Example 1. *Figure 1 shows all possible worlds of an uncertain graph with their existence probabilities. It can be verified that, in each world, the connected component is also the densest subgraph. As Table I shows, the node set* $\{A,B,C,D\}$ *has the maximum expected density (0.38), but it induces a densest subgraph* only *in possible worlds* G_7 *and* G_8 *with low existence probabilities (0.168 and 0.112). Thus, the probability of* $\{A,B,C,D\}$ *inducing a densest subgraph is only 0.28. In contrast, the node set* $\{B,D\}$ *has a lower expected density*

Xiangyu Ke is the corresponding author. Arijit Khan acknowledges support from the Novo Nordisk Foundation grant NNF22OC0072415. Cheng Long is supported by the Ministry of Education, Singapore, under its Academic Research Fund (Tier 1 Award (RG77/21)).

TABLE I: Edge densities in possible worlds (PWs), *expected edge densities* (EEDs) and *densest subgraph probabilities* (DSPs) of node sets in the uncertain graph in Figure 1. The EED of a node set U is the sum of the edge densities of the subgraphs induced by U across all PWs, weighted by their probabilities. The DSP of U is the sum of the probabilities of those PWs where U induces a densest subgraph.

PW:Pr.	{A,B}	{A,C}	{B,D}	{A,B,C}	{A,B,D}	{A,B,C,D}
G_1:0.11	0	0	0	0	0	0
G_2:0.07	**0.5**	0	0	0.33	0.33	0.25
G_3:0.07	0	**0.5**	0	0.33	0	0.25
$\mathbf{G_4}$:**0.25**	0	0	**0.5**	0	0.33	0.25
G_5:0.05	0.5	0.5	0	**0.67**	0.33	0.5
G_6:0.17	0.5	0	0.5	0.33	**0.67**	0.5
$\mathbf{G_7}$:**0.17**	0	**0.5**	**0.5**	0.33	0.33	**0.5**
G_8:0.11	0.5	0.5	0.5	0.67	0.67	**0.75**
EED	0.2	0.2	0.35	0.27	0.37	**0.38**
DSP	0.07	0.24	**0.42**	0.05	0.17	0.28

(0.35), but its probability of inducing a densest subgraph is much higher (0.42), since it induces a densest subgraph in possible worlds G_4 and G_7 with high existence probabilities.

Challenges and our contributions. We formulate and study the novel problem of *most probable densest subgraph* (MPDS) discovery in uncertain graphs: Given an uncertain graph $\mathcal{G}$, find the node set that is the most likely to induce a densest subgraph in $\mathcal{G}$. Our contributions are summarized below.

• **Novel problems:** To the best of our knowledge, the densest subgraph discovery in uncertain graphs has not been investigated before, other than expected edge density [42]. Based on edge density, clique density, and pattern density [5], we propose *densest subgraph probability* as a more sophisticated density metric. We prove that computing the densest subgraph probability is $\#\mathbf{P}$-hard. *We formulate and study the following novel problems of* MPDS *discovery in uncertain graphs* (§ II): MPDS based on edge density, clique density, and pattern density; for each of them, their top-k variants and nucleus densest subgraph (NDS) variants. Real-world applications and case studies demonstrate the usefulness of our novel problems.

• **Efficient approximate solution with end-to-end accuracy guarantees:** In spite of the $\#\mathbf{P}$-hardness of computing the densest subgraph probability, we design an efficient approximation algorithm for the top-k densest subgraphs discovery, with an end-to-end accuracy guarantee. Our solution for edge density-based MPDS is built on independent sampling of possible worlds (e.g., via Monte-Carlo sampling) and, in each of them, efficient enumeration of all edge-densest subgraphs (via [43]). We provide time and space complexity analyses and theoretical accuracy guarantees of our method (§III-A).

• **Extension to other density notions:** Our algorithm can adapt well to clique and pattern densities while ensuring the same accuracy guarantee. Although there exist efficient algorithms to find *one* clique-densest and *one* pattern-densest subgraph in a deterministic graph [5], the problems of enumerating *all* clique- and pattern-densest subgraphs in a deterministic graph have not been studied earlier. However, such enumerations are required in our solution framework. Thus, as additional technical contributions, we develop novel, *exact* algorithms for efficiently enumerating *all* clique- and pattern-densest subgraphs in a deterministic graph (§ III-B, III-C).

• **Practical nucleus densest subgraphs (NDS):** In large graphs, we find that the densest subgraph probability of every possible node set may be quite small, due to the existence of many possible worlds, each having a smaller probability; and any two worlds might not have exactly the same densest subgraph. This defeats our purpose of identifying a node set that induces a *densest* subgraph with a *high probability*. In such cases, we propose to find those nodes which are most likely to form the "nucleus" of various densest subgraphs, i.e., whose containment probability within a densest subgraph is maximized. We develop an approximate solution and present theoretical analyses about its accuracy-efficiency trade-offs. *The novelty of our solution is that, by finding the maximum-sized densest subgraph in each sampled world, we reduce this problem to the closed frequent itemset mining problem, for which efficient algorithms like TFP [44] exist* (§ IV).

• **Experiments and case studies:** Our rigorous experiments (§ VI) show that our MPDS and NDS are different from the existing EDS notion in uncertain graphs (§ VI-B). Also, our methods are efficient even on large graphs (§ VI-E). Our case studies on brain (§ VI-D) and social (§ VI-C) networks demonstrate useful real-world applications of the MPDS.

II. Preliminaries

An uncertain graph $\mathcal{G}$ is a triple (V, E, p), where V is a set of n nodes, $E \subseteq V \times V$ is a set of m undirected unweighted edges, and the function $p : E \to (0, 1]$ assigns a probability of existence to each edge. Following the bulk of the literature on uncertain graphs [26], [29], [30], [45], [46], [47], we assume that the edges exist independent of each other: The uncertain graph $\mathcal{G}$ can be interpreted as a probability distribution over 2^m deterministic instances (possible worlds) $G = (V, E_G) \sqsubseteq \mathcal{G}$ obtained by independently sampling the edges. The probability of a possible world $G = (V, E_G)$ being observed is:

$$\Pr(G) = \prod_{e \in E_G} p(e) \prod_{e \in E \setminus E_G} (1 - p(e)) \tag{1}$$

In the rest of this section, we first revisit several notions of *graph density* [4], [19], [5] in deterministic graphs (§II-A). We next extend these notions to uncertain graphs based on the possible world semantics (§II-B). Then, our novel Most Probable Densest Subgraph (MPDS) problem is formally introduced, together with several practical variants (§II-C). Finally, we discuss the hardness of our problem (§II-D).

A. Density Notions over Deterministic Graphs

1) Edge Density: The edge density [1] measures the average degree per node, which can be used for community detection [48], [3] in social networks.

Definition 1 (Edge Density [1])**.** *The edge density ρ_e of a deterministic graph $G = (V, E)$ is defined as:*

$$\rho_e(G) = \frac{|E|}{|V|} \tag{2}$$

2) Clique Density: An h-clique ($h \geq 2$) is a complete graph of h nodes. The clique density is formally defined below.

Definition 2 (h-Clique Density [19])**.** *Given an integer $h \geq 2$, the h-clique density ρ_h of a deterministic graph $G = (V, E)$, with the number of h-cliques $\mu_h(G)$, is defined as:*

$$\rho_h(G) = \frac{\mu_h(G)}{|V|} \tag{3}$$

Notice that a 2-clique is an edge. Thus, edge density is a special case of clique density when $h = 2$. Clique density benefits in higher-order community discovery and finding subgraphs which are large near-cliques [49], [19].

3) Pattern Density: Given an arbitrary pattern graph, the pattern density measures the average number of such patterns per node occurring in a subgraph.

Definition 3 (Pattern Density [5])**.** *Given a pattern graph ψ, the pattern density ρ_ψ (w.r.t. ψ) of a deterministic graph $G = (V, E)$, with the number of ψ-instances $\mu_\psi(G)$, is:*

$$\rho_\psi(G) = \frac{\mu_\psi(G)}{|V|} \tag{4}$$

Clearly, clique density is a special case of pattern density when the input pattern is a clique. Pattern density can be more expressive in real-world applications. For instance, in the LinkedIn social network, the "employer" nodes (e.g., companies) cannot directly link to the "education" nodes (e.g., universities). Thus, "employer" nodes and "education" nodes never form a clique. However, they can be connected via nodes representing "employee". A subgraph which is dense w.r.t. the "employer-employee1-education-employee2-employer" diamond pattern may identify a group of employees with common work experiences and educational backgrounds.

B. Extending Density Notions to Uncertain Graphs

We define the probability of a node set inducing a densest subgraph in an uncertain graph using possible world semantics.

Definition 4 (Densest Subgraph Probability)**.** *Given an uncertain graph $\mathcal{G} = (V, E, p)$ and a node set $U \subseteq V$, the densest subgraph probability of U, denoted by $\tau(U)$, is the sum of the probabilities of all possible worlds where the subgraph induced by U has the largest density. Formally,*

$$\tau(U) = \sum_{G \sqsubseteq \mathcal{G}} \Pr(G) \times \mathbb{1}\left[\rho(G[U]) = \max_{W \subseteq V} \rho(G[W])\right] \tag{5}$$

The above equation verifies, in each possible world of the uncertain graph $\mathcal{G}$, whether the node set U induces a subgraph with the maximum density. $G[W] = (W, E_G[W])$ denotes the subgraph of G induced by a node set $W \subseteq V$, where $E_G[W] = \{(u, v) \in E_G : u \in W, v \in W\}$. The indicator function $\mathbb{1}[\cdot]$ returns 1 if the inner condition is true (i.e., the subgraph induced by U has the largest density in G), and 0 otherwise. Note that the node set whose induced subgraph has the maximum edge density in G may not be unique. The density metric ρ can follow any of the density notions (§ II-A) based on the real application demand. In the following, without loss of generality, *densest subgraph probability* is coupled with edge density ρ_e by default. For h-clique density ρ_h and pattern density ρ_ψ, we refer to *h-clique densest subgraph probability* τ_h and *pattern densest subgraph probability* τ_ψ respectively.

Example 2. *Figure 2 shows an input uncertain graph and some of its possible worlds. The subgraphs induced by the node set $\{A, C, D\}$ contain a 3-clique (i.e., triangle) only in possible worlds G_1, G_2, G_3, and G_4. In fact, $\{A, C, D\}$ induces 3-clique densest subgraphs in possible worlds G_1, G_2, and G_3, thus the 3-clique densest subgraph probability of $\{A, C, D\}$ is 0.009 + 0.036 + 0.009 = 0.054.*

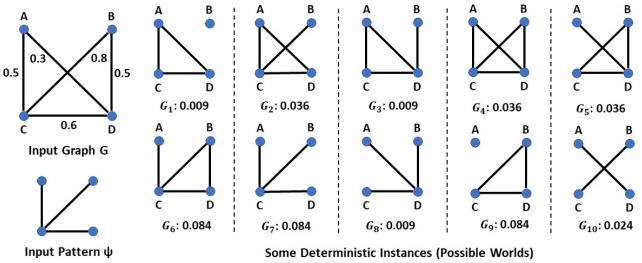

Fig. 2: 3-Clique and pattern densities in an uncertain graph

For the pattern ψ, we notice that the subgraphs induced by node set $\{A, B, C, D\}$ contain ψ only in possible worlds G_2, G_3, G_4, G_5, G_6, G_7, and G_8. Moreover, $\{A, B, C, D\}$ induces the ψ-densest subgraphs in all these six possible worlds, thus the ψ-densest subgraph probability of $\{A, B, C, D\}$ is 0.294.

C. Problem Formulations

We formulate the problem of finding a node set that is the most likely to induce a densest subgraph in an uncertain graph.

Problem 1 (Most Probable Densest Subgraph (MPDS))**.** *Given an uncertain graph $\mathcal{G} = (V, E, p)$, find the node set $U^* \subseteq V$ that has the highest densest subgraph probability.*

$$U^* = \arg\max_{U \subseteq V} \tau(U) \tag{6}$$

The h-Clique-MPDS and Pattern-MPDS problems can be defined analogously. In the following, we provide two other variants of our MPDS problem. First, the user may be interested in exploring more possible choices besides the best node set. Thus, we provide the top-k variant below.

Problem 2 (Top-k Most Probable Densest Subgraphs (Top-k MPDSs))**.** *Given an uncertain graph $\mathcal{G} = (V, E, p)$ and a positive integer k, find the top-k distinct node sets $U_1^*, U_2^*, \ldots, U_k^*$ (where each $U_i^* \subseteq V$, $i \in [1, k]$) having the highest densest subgraph probabilities. Formally,*

$$\begin{aligned} &\tau(U_i^*) \geq \tau(U_{i+1}^*) \quad \forall i \in [1, k) \\ &\tau(U_i^*) \geq \tau(U)\ \forall i \in [1, k]\ \&\ \forall U \subseteq V,\ U \notin \{U_1^*, \ldots, U_k^*\} \end{aligned} \tag{7}$$

Second, in large graphs, we observe that the densest subgraph probability of every node set can be quite small, e.g., below 3.91×10^{-5} in Homo Sapiens, Biomine, and Twitter (§ VI). In such cases, reporting MPDSs contradicts our goal of identifying node sets that can induce densest subgraphs *with high probabilities*. Instead, we find those sets with the highest containment probabilities within a densest subgraph. Such node sets form the "nuclei" of various densest subgraphs across different possible worlds of the uncertain graph.

Definition 5 (Densest Subgraph Containment Probability)**.** *The densest subgraph containment probability $\gamma(U)$ of $U \subseteq V$ is the sum of the probabilities of all possible worlds G of the uncertain graph $\mathcal{G} = (V, E, p)$ such that U is contained in a densest subgraph of G. Formally,*

$$\gamma(U) = \sum_{G \sqsubseteq \mathcal{G}} \Pr(G) \times \mathbb{1}\left[\exists\, U' \supseteq U\ :\ \rho(G[U']) = \max_{W \subseteq V} \rho(G[W])\right]$$

Example 3. *Considering the input uncertain graph in Figure 1, the node set $\{B, D\}$ can induce a densest subgraph*

with probability 0.42 (in possible worlds G_4 and G_7). We notice that $\{B, D\}$ is also contained in densest subgraphs of other possible worlds (G_6 and G_8), even though $\{B, D\}$ alone does not induce densest subgraphs in these worlds. The overall densest subgraph containment probability of $\{B, D\}$ is 0.7 (due to G_4, G_6, G_7, and G_8), which implies that this node set is a critical component in forming densest subgraphs.

There are two caveats for finding the top-k node sets with the highest densest subgraph containment probabilities: (1) A small-sized node set (e.g., a singleton) can also have a high containment probability; however, such sets do not represent meaningful graph communities; (2) If a node set U and one of its supersets U' have equal containment probabilities $\gamma(\cdot)$, then it makes more sense to report U' only (to avoid redundancy). We, therefore, require that all returned node sets must have a minimum specified size and must be closed w.r.t. $\gamma(\cdot)$. A node set is closed w.r.t. $\gamma(\cdot)$ if none of its supersets has the same value of $\gamma(\cdot)$. We now define our NDS problem.

Problem 3 (Top-k Nucleus Densest Subgraphs (NDSs))**.** *Given an uncertain graph $\mathcal{G} = (V, E, p)$ and positive integers k and l_m, let $\mathcal{V}_c^{\geq l_m}$ denote the set of all node sets of size at least l_m that are closed w.r.t. $\gamma(\cdot)$. Find the top-k closed node sets $U_1^*, U_2^*, \ldots, U_k^*$ (where $U_i^* \in \mathcal{V}_c^{\geq l_m}$, $i \in [1, k]$) having the highest densest subgraph containment probabilities. Formally,*

$$\gamma(U_i^*) \geq \gamma(U_{i+1}^*) \quad \forall i \in [1, k)$$
$$\gamma(U_i^*) \geq \gamma(U) \quad \forall i \in [1, k] \;\&\; \forall U \in \mathcal{V}_c^{\geq l_m} \setminus \{U_1^*, \ldots, U_k^*\} \quad (8)$$

Notice that the Top-k MPDS and the NDS problems can be analogously extended to their clique and pattern versions.

D. Hardness

Theorem 1. *Computing the densest subgraph probability of a node set U in an uncertain graph $\mathcal{G} = (V, E, p)$ is $\#\mathbf{P}$-hard.*

Proof. We prove by a reduction from the $\#\mathbf{P}$-hard problem of finding the number of matchings in a graph [45]. A matching in a deterministic graph $G = (V, E)$ is an edge set $M \subseteq E$ without any common nodes.

Consider a deterministic graph $G = (V, E)$. This graph is transformed, by adding two new nodes v_1 and v_2 along with an edge between them, into an uncertain graph $\mathcal{G} = (V \cup \{v_1, v_2\}, E \cup \{(v_1, v_2)\}, p)$, where the probability of each edge is 0.5, except the new edge (v_1, v_2) which has probability 1. Clearly, this reduction takes $\mathcal{O}(|E|)$ time, which is polynomial in the size of G. It can be shown that: • Any possible world $G' \sqsubseteq \mathcal{G}$ with non-zero probability has $\Pr(G') = (0.5)^{|E|}$. • There is a bijection between the set of subsets of E and the set of possible worlds of $\mathcal{G}$ with non-zero probability. • The node set $\{v_1, v_2\}$ induces a densest subgraph in a possible world iff every node has degree at most 1 in that world, i.e., the edges in the world excluding (v_1, v_2) form a matching in G. Thus,

$$\tau(\{v_1, v_2\}) = \sum_{G' \sqsubseteq \mathcal{G}} \Pr(G') \times \mathbb{1}\left[\{v_1, v_2\} = \arg\max_{W \subseteq V} \rho(G'[W])\right]$$
$$= \sum_{G' \sqsubseteq \mathcal{G}} \Pr(G') \times \mathbb{1}\left[\text{each node has degree at most 1 in } G'\right]$$
$$= (0.5)^{|E|} \sum_{G' \sqsubseteq \mathcal{G}: \Pr(G') \neq 0} \mathbb{1}\left[\text{each node has degree at most 1 in } G'\right]$$
$$= (0.5)^{|E|} \sum_{M \subseteq E} \mathbb{1}\left[\text{M is a matching in } G\right]$$

The sum in the last line above is the number of matchings in G. Thus, a solution to our problem on $\mathcal{G}$ provides a solution to the matching counting problem on G. □

Since the computation of $\tau(U)$, for a given U, is $\#\mathbf{P}$-hard, the computations of its generalizations $\tau_h(U)$ and $\tau_\psi(U)$ are also $\#\mathbf{P}$-hard. Thus, finding the node sets with the top-k densest subgraph probabilities, as well as computing the NDS, are also very difficult. *Given such computational challenges, we design approximate algorithms, with end-to-end accuracy guarantees, to find the most probable densest subgraphs in an uncertain graph, based on various graph density notions.*

III. Approximate Solutions for Densest Subgraphs

In this section, we develop approximation algorithms for detecting the top-k MPDSs, along with end-to-end theoretical accuracy guarantees. Our **technical contributions** are as follows: **(1)** We design *novel approximation methods to compute the top-k MPDSs in an uncertain graph for all density notions: edge (§ III-A), clique (§ III-B), and pattern (§ III-C).* **(2)** As building blocks of the algorithms for clique and pattern densities, we also design *novel algorithms to discover all clique and pattern densest subgraphs in a deterministic graph*[1][2](§ III-B and § III-C). **(3)** Additionally, we use these methods to design *approximation algorithms, with end-to-end theoretical quality guarantees, for computing the corresponding NDS (§ IV).*

A. Top-k MPDS: Approximate Algorithm

The proposed solution (Algorithm 1) runs θ independent iterations as follows: Sample a possible world $G \sqsubseteq \mathcal{G}$ and find *all* the node sets inducing the densest subgraphs in G (Line 5). $\widehat{\tau}(U)$ denotes the estimated densest subgraph probability, which is computed as the average frequency that a node set U induces a densest subgraph across θ rounds. Finally, we return the top-k node sets having the highest $\widehat{\tau}(\cdot)$.

Lemma 1. *$\widehat{\tau}(U)$ is an unbiased estimator for $\tau(U)$. Formally, $\mathbb{E}[\widehat{\tau}(U)] = \tau(U)$.*

Proof. Let $X_i(U)$ be a binary random variable denoting whether U induces a densest subgraph in the i^{th} possible world; thus $\widehat{\tau}(U) = \frac{1}{\theta}\sum_{i=1}^{\theta} X_i(U)$. Clearly, $\mathbb{E}[X_i(U)] = \Pr(X_i[U] = 1) = \tau(U)$, and hence $\mathbb{E}[\widehat{\tau}(U)] = \tau(U)$. □

The unbiasedness ensures that the estimated $\widehat{\tau}(U)$ goes closer to the true value $\tau(U)$ as the sample size θ increases.

The technique in [43] for computing all densest subgraphs in a deterministic graph (Line 5) involves reducing the graph to its $\lceil\tilde{\rho}\rceil$-core [51], where $\tilde{\rho}$ is a lower bound on the maximum edge density ρ_e^* of any subgraph. This is followed by computing ρ_e^* using the state-of-the-art Goldberg's algorithm [1]. During each iteration of its binary search, the Goldberg's algorithm tries to find a subgraph with density larger than a guessed value α by computing the minimum cut in a flow

[1]Due to the extra nodes for cliques/patterns in the flow network, the definitions and theorems do not trivially follow [43]; more details can be found in the remark in § III-B

[2]Our empirical study [50] validates that considering *all* densest subgraphs can significantly outperform (e.g., up to 20× in LastFM) the method that considers only one randomly chosen densest subgraph.

Algorithm 1 Top-k MPDS estimation

Input: Uncertain graph $\mathcal{G} = (V, E, p)$, positive integer k, and number of samples θ
Output: (Approximate) Top-k MPDS
1: **for all** $U \subseteq V$ **do**
2: $\quad\widehat{\tau}(U) \leftarrow 0$
3: **for** $i = 1$ **to** θ **do**
4: $\quad$Sample a possible world $G \sqsubseteq \mathcal{G}$
5: $\quad S \leftarrow$ All densest subgraphs in G via [43]
6: $\quad$**for all** $U \in S$ **do**
7: $\quad\quad\widehat{\tau}(U) \leftarrow \widehat{\tau}(U) + \frac{1}{\theta}$
8: **return** Top-k U's having the highest $\widehat{\tau}(U)$

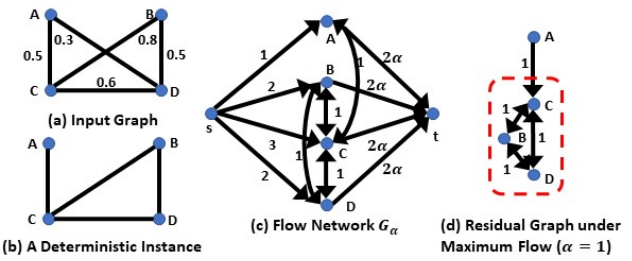

Fig. 3: Finding all densest subgraphs in a possible world

network parameterized by α. Once ρ_e^* is found, all densest subgraphs are enumerated by traversing the strongly connected components (SCCs) in the residual graph (under a maximum flow) of the flow network with $\alpha = \rho_e^*$; the details can be found in [43] and in the example below.

Example 4. *We shall compute all densest subgraphs in a possible world G (Figure 3(b)) of an uncertain graph $\mathcal{G}$ ((Figure 3(a)). A flow network G_α (Figure 3(c)) is constructed as follows. (1) Add a source node s and a sink node t. (2) If an edge (u, v) exists in G, add an edge from u to v and one from v to u in G_α, both with capacity 1. (3) Add an edge from s to each node v in G with capacity equal to the degree of v in G. (4) Add an edge from each node in G to t with capacity 2α. Goldberg's algorithm [1] conducts a binary search with $[0, m]$ as the initial range of α. In each iteration, it guesses an α and computes the maximum flow (minimum cut) in the flow network. Once terminated, the optimal density is assigned to be $\rho^* = \alpha$. In this example, we get $\rho^* = 1$ and a densest subgraph $\{A, B, C, D\}$ (which corresponds to the minimum cut). To find the other densest subgraphs, we create the residual graph ((Figure 3(d)) by removing all the edges with zero residual capacity. The densest subgraphs are enumerated by exploring the SCCs in this residual graph. In this case, we find one additional densest subgraph $\{B, C, D\}$.*

Space complexity. The majority of the memory is consumed by the flow network in each iteration of the binary search, and hence the overall space complexity is $\mathcal{O}(m + n)$.

Time complexity. Recall that we sample θ possible worlds. The computation of the $\lceil\tilde{\rho}\rceil$-core of each possible world takes $\mathcal{O}(m)$ time [51]. Let n_c and m_c denote the number of nodes and edges respectively in the $\lceil\tilde{\rho}\rceil$-core of a sampled possible world $G \sqsubseteq \mathcal{G}$. As shown in [43], the computation of ρ_e^* takes $\mathcal{O}\left(n_c m_c \log\left(\frac{n_c^2}{m_c}\right)\right)$ time, while the enumeration of the densest subgraphs takes $\mathcal{O}(L)$ time per subgraph, where L is the number of nodes in that densest subgraph (note that $L \leq n$). Denoting respectively by n_c^*, m_c^*, d^*, and L^* the maximum number of nodes, edges, densest subgraphs, and nodes in a densest subgraph in any possible world, the overall time complexity of our algorithm is $\mathcal{O}\left(\theta\left(m + n_c^* m_c^* \log\left(\frac{n_c^{*2}}{m_c^*}\right) + d^* L^*\right)\right)$. Practically, $n_c^* \ll n$, $m_c^* \ll m$ and $L^* \ll n$, as validated in our experiments (§ VI). For instance, $\frac{n_c^*}{n} = 2.45 \times 10^{-4}$, $\frac{L^*}{n} = 1.8 \times 10^{-4}$, $\frac{m_c^*}{m} = 5.43 \times 10^{-3}$, and $d^* = 1$ in our large Twitter dataset, making Algorithm 1 efficient even with large-scale graphs.

Accuracy guarantee. We theoretically analyze the sample size θ to return the true top-k node sets with a high probability.

Theorem 2. *Let $V_1, \ldots, V_k$ denote the true top-k node sets having the highest densest subgraph probabilities, and let CV denote the set of candidate node sets after θ rounds. Then,*

$$\Pr\left(\{V_1, \ldots, V_k\} \subseteq CV\right) \geq 1 - \sum_{i=1}^{k} \left(1 - \tau(V_i)\right)^\theta \tag{9}$$

Proof. Since we compute all densest subgraphs in each of θ independently sampled possible worlds, $\Pr\left(V_i \notin CV\right) = \left(1 - \tau(V_i)\right)^\theta \ \forall i \in \{1, \ldots, k\}$. From the union bound,

$$\Pr\left(\{V_1, \ldots, V_k\} \subseteq CV\right) = 1 - \Pr\left(\exists i \in \{1, \ldots, k\} : V_i \notin CV\right)$$
$$\geq 1 - \sum_{i=1}^{k} \Pr\left(V_i \notin CV\right) = 1 - \sum_{i=1}^{k} \left(1 - \tau(V_i)\right)^\theta$$

From Theorem 2, if the densest subgraph probabilities of the true top-k node sets and the sample size θ are reasonably large, they are all highly likely to be included in the candidate node set, which is necessary for all of them to be returned.

Theorem 3. *Let $V_1, \ldots, V_{k+1}$ denote the true top-$(k+1)$ node sets having the highest densest subgraph probabilities, and let CV denote the set of candidate node sets after θ rounds. Define $mid = \frac{1}{2}\left[\tau\left(V_k\right) + \tau\left(V_{k+1}\right)\right]$ and*

$$d_U = \begin{cases} \tau(U) - mid & \text{if } U \in \{V_1, \ldots, V_k\} \\ mid - \tau(U) & \text{otherwise} \end{cases} \tag{10}$$

Then, the probability that $V_1, \ldots, V_k$ are returned by Algorithm 1 is at least

$$\left[1 - \sum_{i=1}^{k} \left(1 - \tau(V_i)\right)^\theta\right]\left[1 - \sum_{U \in CV} \exp\left(-2 d_U^2 \theta\right)\right] \tag{11}$$

Proof. Let $CV' = CV \setminus \{V_1, \ldots, V_k\}$. We have:

$$\Pr(V_1, \ldots V_k \text{ are returned}) \geq \Pr(\{V_1, \ldots, V_k\} \subseteq CV) \times$$
$$\Pr\left(\left(\bigwedge_{U \in \{V_1, \ldots, V_k\}} \widehat{\tau}(U) > mid\right) \wedge \left(\bigwedge_{U \in CV'} \widehat{\tau}(U) < mid\right)\right) \tag{12}$$

Now, using the union bound and Hoeffding's inequality,

$$\Pr\left(\left(\bigwedge_{U \in \{V_1, \ldots, V_k\}} \widehat{\tau}(U) > mid\right) \wedge \left(\bigwedge_{U \in CV'} \widehat{\tau}(U) < mid\right)\right)$$
$$= 1 - \Pr\left(\left(\bigvee_{U \in \{V_1, \ldots, V_k\}} \widehat{\tau}(U) \leq mid\right) \vee \left(\bigvee_{U \in CV'} \widehat{\tau}(U) \geq mid\right)\right)$$
$$\geq 1 - \sum_{U \in \{V_1, \ldots, V_k\}} \Pr\left(\widehat{\tau}(U) \leq mid\right) - \sum_{U \in CV'} \Pr\left(\widehat{\tau}(U) \geq mid\right)$$
$$= 1 - \sum_{U \in \{V_1, \ldots, V_k\}} \Pr\left(\widehat{\tau}(U) - \tau(U) \leq -d_U\right) - \sum_{U \in CV'} \Pr\left(\widehat{\tau}(U) - \tau(U) \geq d_U\right)$$
$$\geq 1 - \sum_{U \in CV} \exp\left(-2 d_U^2 \theta\right) \tag{13}$$

Algorithm 2 Find all clique-densest subgraphs

Input: Deterministic graph $G = (V, E)$, positive integer h
Output: All h-clique densest subgraphs in G
1: $\tilde{\rho} \leftarrow$ Density returned by the peeling method [19], [5]
2: $G_c \leftarrow (\lceil \tilde{\rho} \rceil, h)$-core of G [5]
3: $\Lambda \leftarrow$ All $(h-1)$-cliques contained in h-cliques in G_c [54]
4: $\rho_h^* \leftarrow \max_{S \subseteq V} \rho_h(S)$ [55]
5: $\mathcal{H} \leftarrow$ Flow network as in [20]
6: $f^* \leftarrow$ Maximum flow in $\mathcal{H}$
7: $\mathcal{C} \leftarrow$ SCCs of the residual graph $\mathcal{H}_{f^*}$, excluding those of s and t
8: **return** Algorithm 3 $(\emptyset, \mathcal{C}, V)$

Algorithm 3 Enumerate all clique densest subgraphs

Input: Component sets $\mathcal{C}_1$ and $\mathcal{C}_2$, node set V
Output: All clique-densest subgraphs
1: $R \leftarrow \emptyset$
2: **if** $\mathcal{C}_1 \neq \emptyset$ **then**
3: $\quad R \leftarrow R \cup \left(\bigcup_{C \in \mathcal{C}_1 \cup des(\mathcal{C}_1)} C \cap V \right)$
4: **for all** $C \in \mathcal{C}_2$ **do**
5: $\quad$ **if** $C \cap V \neq \emptyset$ **then**
6: $\quad\quad \mathcal{C}_2 \leftarrow \mathcal{C}_2 \setminus \{C\}$
7: $\quad\quad S \leftarrow$ Algorithm 3 $(\mathcal{C}_1 \cup \{C\}, \mathcal{C}_2 \setminus (des(C) \cup anc(C)), V)$
8: $\quad\quad R \leftarrow R \cup S$
9: **return** R

Finally, plugging (9) and (13) into (12), we obtain (11). □

From Theorem 3, if the densest subgraph probabilities of the true top-k node sets are reasonably large in contrast to the others and if the sample size θ is sufficiently large, the true top-k sets are returned by Algorithm 1 with a high probability.

Remarks. (1) Notice that the algorithmic framework and accuracy guarantees can be adapted to solve the top-k Clique-MPDS (resp. Pattern-MPDS) problems. However, we need to develop an efficient algorithm for detecting *all* clique (resp. pattern)-densest subgraphs in each sampled possible world (Line 5 of Algorithm 1), which is our *novel technical contribution* in § III-B (resp. § III-C). **(2)** Our analyses are based on the assumption that we use *Monte Carlo* to sample possible worlds. There also exist other sampling techniques such as *Lazy Propagation* [52] and *Recursive Stratified Sampling* [53]. We empirically show in our extended version [50] that, for our problem, these three sampling strategies result in *similar sample sizes* θ and have *comparable running times*, while *Monte Carlo* consumes *much less memory*.

B. h-Clique-MPDS: Approximate Algorithm

Inspired by [43], we develop a novel, exact, and efficient solution to discover *all* clique-densest subgraphs in a deterministic graph (Algorithm 2). *This is a novel problem, and no existing work has studied it. Therefore, Algorithm 2 is one of our novel technical contributions*. In the following, we first revisit the concepts of clique degree (Definition 6) and clique-based core (Definition 7) in deterministic graphs. Then, we illustrate the technical details and the intuitions of our algorithm, together with a running example. Finally, we provide theoretical analyses about its efficiency and correctness.

Definition 6 (h-Clique Degree [5])**.** *The h-clique degree ($h \geq 2$) of a node v in a deterministic graph G, denoted by $deg_G(v, h)$, is the number of h-cliques in G containing v.*

Definition 7 ((k, h)-Core [5])**.** *Given a deterministic graph G and two integers $h \geq 2$ and $k \geq 0$, the (k, h)-core of G, denoted by $\mathcal{R}_k$, is the largest subgraph of G such that, for every node v in $\mathcal{R}_k$, $deg_{\mathcal{R}_k}(v, h) \geq k$.*

Armed with these definitions, we proceed to the details of Algorithm 2, which consists of two general steps: **(1)** The technique in [55] is applied to compute the maximum density of any subgraph of G. **(2)** A flow network $\mathcal{H}$ is constructed following [20], [43]. The SCCs of the residual graph under a maximum flow in $\mathcal{H}$ indicate all densest subgraphs of G.

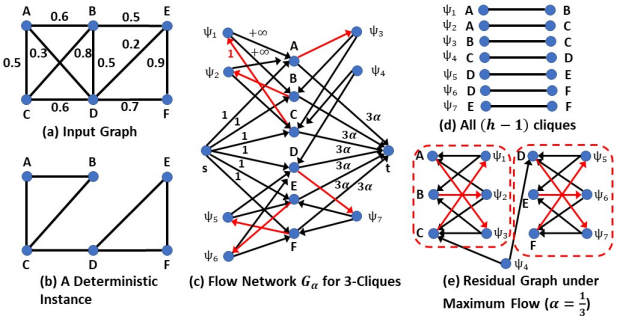

Fig. 4: Finding all 3-clique densest subgraphs in a possible world

In Line 1, it runs the peeling method of [19], which iteratively removes the node with the smallest h-clique degree and returns the maximum density among all the resultant subgraphs, denoted by $\tilde{\rho}$. Then, in Line 2, it replaces G with its $(\lceil \tilde{\rho} \rceil, h)$-core, i.e., the subgraph induced by those nodes which have h-clique degree at least $\tilde{\rho}$. After that, Line 3 computes the set Λ of all $(h-1)$-cliques contained in h-cliques in G, which are enumerated using the method in [54]. Line 4 computes ρ_h^*, the maximum h-clique density of any subgraph, by the method in [55], which iteratively computes a (predicted) clique-densest subgraph via optimizing a convex program, till the computed subgraph is deemed to be indeed clique-densest. After that, the clique density of the computed subgraph is returned.

Next, Line 5 constructs a flow network $\mathcal{H}$ [20], [5], which contains one node for each $(h-1)$-clique in Λ and one for each node in V, in addition to a source node s and a sink node t (see our extended version [50] for the pseudocode). Once $\mathcal{H}$ is constructed, Algorithm 2 computes a maximum flow f^* in $\mathcal{H}$ (Line 6) and then identifies the strongly connected components (SCCs) of the residual graph $\mathcal{H}_{f^*}$ of $\mathcal{H}$ under f^* (Line 7) after removing the edges with zero residual capacity.

Finally, in Line 8, Algorithm 3 enumerates one densest subgraph of G for every value of $C \cup des(C)$, where C is an SCC of $\mathcal{H}_{f^*}$, and the set $des(C)$ (resp. $anc(C)$) denotes the set of SCCs having a directed path from (resp. to) C in the SCC graph of $\mathcal{H}_{f^*}$. The detailed theoretical analyses for Algorithms 2 and 3 are given in our extended version [50].

Example 5. *We shall compute all h-clique densest subgraphs ($h = 3$) in a possible world G (Figure 4(b)) of an uncertain graph $\mathcal{G}$ ((Figure 4(a)). The maximum 3-clique density ρ_h^* of any subgraph of G can be easily computed as $\frac{1}{3}$. A flow network G_α is constructed as in Figure 4(c). Instead of directly adding edges between nodes as for edge density (Example 4), a new set of nodes representing the $(h-1)$-cliques is added.*

A $(h-1)$-clique node ψ_i has a directed edge to each node contained in this $(h-1)$-clique, with infinite capacity. If a node v forms an h-clique with the $(h-1)$-clique ψ_i, a directed edge from v to ψ_i is added with capacity 1. For simplicity, we only show the capacities of the edges entering and leaving ψ_1 in Figure 4(c). In this example, the $(h-1)$-cliques are all edges in the possible world, as shown in Figure 4(d). After plugging in $\rho_h^* = \frac{1}{3}$ and computing the maximum flow, we identify a 3-clique densest subgraph $\{A, B, C, D, E, F\}$, and obtain a residual graph as shown in Figure 4(e). The remaining 3-clique densest subgraphs are $\{A, B, C\}$ and $\{D, E, F\}$. Each of them corresponds to an SCC of the residual graph.

Remark. Our Algorithm 2 for computing all clique-densest subgraphs has similarities to the method of computing all edge-densest subgraphs in [43]. *However, there are also major differences from [43]:* As demonstrated in Example 5, our flow network $\mathcal{H}$ has one additional node for each $(h-1)$-clique in Λ (in addition to one for each node in V as in [43]), and the edges are from nodes in V to nodes in Λ (unlike [43], where the edges only exist between nodes in V). Thus, some non-trivial additions[3] need to be incorporated into the definitions and proofs in [43] to prove the correctness of our Algorithms 2 and 3. *This forms one of our novel technical contributions.*

Space complexity. Let G_c be the $(\lceil\tilde{\rho}\rceil, h)$-core in Lines 1-2 of Algorithm 2, with n_c and m_c the corresponding node and edge counts respectively. As each h-clique of G_c contains h distinct $(h-1)$-cliques, $|\Lambda| = \mathcal{O}\left(h\mu_h(G_c)\right)$, where $\mu_h(G_c)$ is the number of h-cliques in G_c. Thus, the number of nodes in $\mathcal{H}$ is $\mathcal{O}\left(n_c + h\mu_h(G_c)\right)$ and the number of edges is $\mathcal{O}\left(n_c + \sum_{v\in V} deg_{G_c}(v,h) + (h-1)h\mu_h(G_c)\right) = \mathcal{O}\left(n_c + h^2\mu_h(G_c)\right)$. Since these consume the most memory, the space complexity of Algorithm 2 is $\mathcal{O}\left(n_c + h^2\mu_h(G_c)\right)$.

When we adapt Algorithm 1 for h-Clique-MPDS, in addition to the memory required for storing the uncertain graph, the majority of the memory is consumed by Line 5, which invokes Algorithm 2. Denoting by μ_h^* the maximum number of h-cliques in the $(\lceil\tilde{\rho}\rceil, h)$-core of any possible world of $\mathcal{G}$, the overall space complexity of our method is $\mathcal{O}\left(m + n + h^2\mu_h^*\right)$.

Time complexity. For Lines 1-3 in Algorithm 2, the major step is enumerating all h-cliques in G, which takes $\mathcal{O}\left(hm\left(\frac{1}{2}\cdot\mu_h(G)\right)^{h-2}\right)$ time, where $\mu_h(G)$ is the number of h-cliques in G [54]. If T denotes the number of iterations involved in computing ρ_h^* using [55], the running time of Line 4 consists of optimizing the convex program and computing the maximum flow in each iteration [55], and requires $\mathcal{O}\left(2^T h\mu_h(G_c) + T\left(n_c h\mu_h(G_c) + n_c^3\right)\right)$ time, where n_c is as defined above. Lines 5-6 can be done in $\mathcal{O}\left(\left(n_c h\mu_h(G_c) + n_c^3\right)\right)$ time [5]. Line 7 takes $\mathcal{O}\left(n_c + h^2\mu_h(G_c)\right)$ time, as it involves finding the SCCs of $\mathcal{H}_{f^*}$, whose node and edge counts are stated above. In Line 8, each densest subgraph is enumerated exactly once (as proved in our extended version [50]), and each subgraph enumeration takes time linear in the corresponding number of nodes.

[3]In our extended version [50], Definitions 10-11 and the proofs of Lemmas 9-10 are different from [43]. Moreover, Lemma 7 is newly derived and serves as a critical reason for not considering the SCC of the sink node.

Algorithm 4 Find all pattern-densest subgraphs

Input: Deterministic graph $G = (V, E)$, pattern $\psi = (V_\psi, E_\psi)$
Output: All pattern-densest subgraphs w.r.t. ψ in G
1: $\tilde{\rho} \leftarrow$ Density returned by the peeling method [5]
2: $G_c \leftarrow (\lceil\tilde{\rho}\rceil, \psi)$-core of G [5]
3: $\Lambda \leftarrow$ All ψ-instances in G_c [56]
4: $\rho_\psi^* \leftarrow \max_{S\subseteq V} \rho_\psi(S)$ [55]
5: $\mathcal{H} \leftarrow$ Flow network as in [5]
6: $f^* \leftarrow$ Maximum flow in $\mathcal{H}$
7: $\mathcal{C} \leftarrow$ SCCs of the residual graph $\mathcal{H}_{f^*}$, excluding those of s and t
8: **return** Algorithm 3 $(\emptyset, \mathcal{C}, V)$

Denoting respectively by n_c^*, d^*, L^*, and T^*, the maximum number (in the $(\lceil\tilde{\rho}\rceil, h)$-core of any possible world) of nodes, densest subgraphs, nodes in a densest subgraph and iterations of [55] to compute ρ_h^*, and by μ_h^* the maximum number of h-cliques in any possible world, the overall time complexity of our method is $\mathcal{O}\left(\theta\left(hm\left(\frac{1}{2}\cdot\mu_h^*\right)^{h-2} + 2^{T^*}h\mu_h^* + T^*\left(n_c^* h\mu_h^* + {n_c^*}^3\right) + d^* L^*\right)\right)$. Practically, $n_c^* \ll n$ and T^* is very small, as validated in our experiments (§ VI). For instance, $T^* = 11$, $\frac{n_c^*}{n} = 4.731\times10^{-4}$, $\frac{L^*}{n} = 2.049\times10^{-5}$, $\frac{\mu_h^*}{m} = 0.181$, and $d^* = 1$ for our large Twitter dataset, making our algorithm quite efficient with large-scale graphs.

Accuracy guarantee. We briefly show (and in details in our extended version[50]) that Algorithm 2 correctly computes all clique-densest subgraphs in a deterministic graph. Thus, our overall accuracy guarantees for finding the top-k h-Clique-MPDSs in an uncertain graph remain the same as in §III-A.

Theorem 4. *Algorithm 2 enumerates each h-clique densest subgraph of a deterministic graph G exactly once.*

Proof Sketch. Lines 1-2 of Algorithm 2 are justified by the fact that the densest subgraph is in the $(\lceil\rho_h^*\rceil, h)$-core, and hence in the $(\lceil\tilde{\rho}\rceil, h)$-core [5]. The correctness of Line 4 follows from [55]. The main idea behind the remaining lines is that all h-clique densest subgraphs of G are hidden in the SCCs of the residual graph $\mathcal{H}_{f^*}$ of $\mathcal{H}$ under a maximum flow f^*. Any h-clique densest subgraph of G constitutes a minimum s-t cut in $\mathcal{H}$. Thus, this subgraph has no outgoing edge in $\mathcal{H}_{f^*}$. □

C. Pattern-MPDS: Approximate Algorithm

Algorithm 4 for finding *all* pattern-densest subgraphs (w.r.t. a given pattern $\psi = (V_\psi, E_\psi)$) is inspired by [43]. As earlier, *finding all pattern-densest subgraphs in a deterministic graph is a novel problem, and Algorithm 4 is a novel contribution.*

Algorithm 4 is similar to Algorithm 2 (§ III-B); in fact, the (k,h)-core (Definition 7) can be extended to the (k,ψ)-core (Line 2), and ρ_ψ^* is computed in Line 4 by extending [55]. In Line 3, Λ refers to the set of all ψ-instances in G instead of cliques, which is enumerated using [56]. Moreover, the flow network $\mathcal{H}$ (constructed as in [5]; the pseudocode is included in our extended version [50]) contains one node for each group of ψ-instances with a common node set, instead of one for each instance, to reduce the memory footprint and running time. This forms the main difference between our method and the one in [43], resulting in some non-trivial additions which constitute one of our novel contributions (see [50]).

Accuracy guarantee. We prove in our extended version [50] that Algorithm 4 correctly computes pattern-densest subgraphs w.r.t. ψ in a deterministic graph. The main difference is in the derivation of the capacity of a minimum cut in $\mathcal{H}$, which is quite different from the one in § III-B as mentioned above. Finally, since Algorithm 4 correctly computes all pattern-densest subgraphs w.r.t. ψ in a deterministic graph, our overall accuracy guarantees for finding the top-k Pattern-MPDS in an uncertain graph remain the same as in §III-A.

Space complexity. Let G_c be the $(\lceil\tilde{\rho}\rceil, \psi)$-core in Lines 1-2 of Algorithm 4, with n_c and m_c the corresponding node and edge counts respectively. Clearly $|\Lambda| = \mathcal{O}(\mu_\psi(G_c))$, where $\mu_\psi(G_c)$ is the number of ψ-instances in G_c. Thus, the number of nodes in $\mathcal{H}$ is $\mathcal{O}(n_c + \mu_\psi(G_c))$ and the number of edges is $\mathcal{O}(n_c + |V_\psi|\,\mu_\psi(G_c))$. Also, computing ρ^*_ψ (Line 4) requires $\mathcal{O}(n_c + |\Lambda|) = \mathcal{O}(n_c + \mu_\psi(G_c))$ space [5]. Since these constitute most of the memory consumed, the total space complexity of Algorithm 4 is $\mathcal{O}(n_c + |V_\psi|\,\mu_\psi(G_c))$.

When we adapt Algorithm 1 for Pattern-MPDS, in addition to the memory required for storing the uncertain graph, the majority of the memory is consumed by Line 5, which invokes Algorithm 4. Denoting by μ^*_ψ the maximum number of ψ-instances in the $(\lceil\tilde{\rho}\rceil, h)$-core of any possible world of $\mathcal{G}$, the overall space complexity is $\mathcal{O}\left(m + n + |V_\psi|\,\mu^*_\psi\right)$.

Time complexity. Assume that the enumeration of all ψ-instances in a possible world takes $\mathcal{O}(t_\psi)$ time. By a similar analysis as in § III-B, denoting respectively by n^*_c, d^*, L^*, μ^*_ψ, and T^*, the maximum number (in the $(\lceil\tilde{\rho}\rceil, \psi)$-core of any possible world) of nodes, densest subgraphs, nodes in a densest subgraph, ψ-instances, and iterations of [55] to compute ρ^*_ψ, the overall time complexity of our method is $\mathcal{O}\left(\theta\left(t_\psi + 2^{T^*}|V_\psi|\,\mu^*_\psi + T^*\left(n^*_c\mu^*_\psi + n^{*3}_c\right) + d^*L^*\right)\right)$.

Remark. For larger graphs and bigger patterns ψ, we find that the enumeration of all ψ-instances (which is necessary to compute the densest subgraphs in a possible world) can be expensive. In such cases, we resort to a heuristic method in which we enumerate some reasonably dense subgraphs (instead of all densest ones) using [5]. Specifically, we use a method different from Algorithm 4, which runs core decomposition w.r.t. ψ. If k_{max} denotes the maximum core number, then the (k_{max}, ψ)-core is a reasonably dense subgraph. In particular, the (k_{max}, ψ)-core's density is at least $\frac{1}{|V_\psi|}$ times the maximum density of any subgraph [5]. Based on this, we return the (k_{max}, ψ)-core and all intermediate subgraphs (obtained during core decomposition) having greater densities. Experimental results [50] show that this heuristic method yields good-quality solutions with higher efficiency.

IV. NDS: Approximate Solution

We convert the NDS (nucleus densest subgraphs) problem into the widely-studied closed frequent itemset mining problem and develop an *approximate method* (Algorithm 5) to find the top-k NDS for all three notions of density: edge, clique, and pattern density. The algorithm first runs θ independent rounds: Sample a possible world $G \sqsubseteq \mathcal{G}$ and insert, into the set of candidate node sets CV, the maximum-sized densest subgraph of G[4]. For a node set $U \subseteq V$, let $\widehat{\gamma}(U)$ denote the estimated densest subgraph containment probability of U, which is computed as the fraction of node sets in CV which contain U. Then a closed frequent itemset mining algorithm (e.g., TFP [44]) is applied to compute the top-k closed node sets in CV of size at least l_m having the largest values of $\widehat{\gamma}(\cdot)$. A node set is closed w.r.t. $\widehat{\gamma}(\cdot)$ if it has no superset with the same value of $\widehat{\gamma}(\cdot)$. Here, l_m is a user input decided based on the minimum desired size of a returned subgraph.

Algorithm 5 Estimate all NDS in an uncertain graph

Input: Uncertain graph $\mathcal{G} = (V, E, p)$, positive integers k and l_m, no. of samples θ
Output: (Approximate) NDS
1: $CV \leftarrow \emptyset$
2: **for** $i = 1$ **to** θ **do**
3: Sample a possible world $G \sqsubseteq \mathcal{G}$
4: $S \leftarrow$ Maximum-sized densest subgraph in G
5: $CV \leftarrow CV \cup \{S\}$
6: **return** TFP(CV, k, l_m) [44]

The maximum-sized densest subgraph in a deterministic graph (Line 4) can be computed using parts of the methods in § III. For edge density, we terminate after computing the SCCs of the residual graph under a maximum flow [43]. For clique and pattern densities, we terminate after computing the value of the maximum density of a subgraph, since we also get the maximum-sized densest subgraph in this process [55].

Space complexity. The major memory cost is due to the flow network in each iteration of Algorithm 5. Therefore, the overall space complexity is the same as in § III.

Time complexity. The time complexity is similar to the ones in § III, plus that for computing the closed frequent node sets by TFP, which is reasonable in our experiments (§ VI-F).

Accuracy guarantee.

Theorem 5. *Let $V_1, \ldots, V_{k+1}$ denote the true top-$(k+1)$ closed node sets of size at least l_m having the highest densest subgraph containment probabilities, and let CV denote the set of candidate node sets after θ rounds. Define $mid = \frac{1}{2}\left[\gamma(V_k) + \gamma(V_{k+1})\right]$ and*

$$d_U = \begin{cases} \gamma(U) - mid & \text{if } U \in \{V_1, \ldots, V_k\} \\ mid - \gamma(U) & \text{otherwise} \end{cases} \tag{14}$$

For each $i \in [1, k]$, let $\mathbf{G}(V_i)$ denote the set of all possible worlds of $\mathcal{G}$ whose densest subgraphs contain V_i. Define $\mathbb{G} = \bigcup_{i=1}^{k} \mathbf{G}(V_i)$ and $\mathcal{CV}$ as the set of all closed node sets w.r.t. $\widehat{\gamma}(\cdot)$ of size at least l_m. Then, the probability that $V_1, \ldots, V_k$ are returned by Algorithm 5 is at least

$$\left[1 - \sum_{G \in \mathbb{G}} \left(1 - \Pr(G)\right)^\theta\right]\left[1 - \sum_{U \in \mathcal{CV}} \exp\left(-2d_U^2\theta\right)\right] \tag{15}$$

The proof is given in our extended version [50]. From Theorem 5, if the densest subgraph containment probabilities of the true top-k node sets are reasonably larger than the other

[4] By a trivial generalization of [57] to all density notions, the union of the node sets of all densest subgraphs of a deterministic graph G induces the maximum-sized (w.r.t. node count) densest subgraph in G. Thus, a node set is contained in a densest subgraph of G if and only if it is contained in the maximum-sized densest subgraph of G.

closed node sets w.r.t. $\widehat{\gamma}(\cdot)$ of size at least l_m, and if the sample size θ is sufficiently large, the true top-k sets are returned by Algorithm 5 with a high probability.

V. Related Work

We first revisit the densest subgraph problem in deterministic graphs. Then, we discuss the maximum expected density in uncertain graphs. Finally, we state several close notions for cohesive and dense substructures in uncertain graphs.

Densest subgraph in a deterministic graph. Given an undirected, unweighted, deterministic graph, the original densest subgraph (DS) problem [1] finds a subgraph with the highest edge-density, exact solutions to which are based on min-cuts in flow-networks [1], [5] and linear programming [1], [2]. To mitigate high computation costs, researchers proposed approximate algorithms with theoretical guarantees, e.g., [2], [5], [58], [59]. Variants of the edge-density-based DS problem were also studied, such as triangle-density, clique-density, pattern-density, and edge-surplus based DS [5], [20], [55], [19], [3], size-bounded DS [60], top-k DS maintenance on dynamic graphs [61], [58], [59], locally DS [62], density-friendly graph decomposition [63], [64], DS on directed [65], bipartite [66], multilayer graphs [67], etc. For surveys and tutorials, we refer to [68], [4]. Enumerating all the densest subgraphs based on edge-density in a deterministic graph has been recently studied in [43], which we use as a subroutine to find the MPDS of an uncertain graph in our problem. We notice that the problems of enumerating all clique-DS and pattern-DS in a deterministic graph were not studied in the literature. Thus, as additional technical contributions, we develop novel, exact algorithms for efficiently enumerating all clique- and pattern-DS in a deterministic graph, and use them as subroutines to respectively find the h-Clique- and the Pattern-MPDS of an uncertain graph in our problem.

Expected edge densest subgraph. The expected edge density of a node set U in an uncertain graph is the expectation of the edge density of the subgraph induced by U across all possible worlds. Zou [42] designed a polynomial-time algorithm to find the subgraph with the maximum expected edge density in an uncertain graph using maximum flow techniques. As shown in Example 1 and our experiments (§VI-B and §VI-C), the expected edge densest subgraph is different from the MPDS: a subgraph of an uncertain graph having the maximum expected edge density may induce densest subgraphs *only in a few* possible worlds of the graph. Such a subgraph can be large with many low-probability edges or loosely connected nodes.

Core and truss decompositions in uncertain graphs. As cohesive and dense substructures finding, core and truss decompositions are popular. The k-core (resp. k-truss) of a graph is a maximal subgraph in which every node is connected to at least k other nodes (resp. each edge participates in at least $(k-2)$ triangles). They have been extended to uncertain graphs [35], [69], [70], [71], [36], [72], [73]. The innermost cores and trusses have been used in applications such as task-driven team formation due to their higher densities [36], [35]. However, unlike the MPDS, their returned node set may not be most likely to induce a densest subgraph in an uncertain graph (§VI-B and §VI-C).

TABLE II: Characteristics of our datasets

Name	n	m	Type	Edge Prob: Mean, St. Dev., Quart.
Karate Club	34	78	Social	0.25, 0.09, {0.18, 0.26, 0.33}
Intel Lab	54	969	Device	0.33, 0.19, {0.16, 0.27, 0.44}
LastFM	6 899	23 696	Social	0.33, 0.19, {0.16, 0.27, 0.44}
Homo Sapiens	18 384	995 916	Bio	0.32, 0.21, {0.18, 0.24, 0.34}
Biomine	1 045 414	6 742 939	Bio	0.27, 0.21, {0.12, 0.22, 0.36}
Twitter	6 294 565	11 063 034	Social	0.14, 0.10, {0.10, 0.10, 0.19}
Friendster	65 608 366	1 806 067 135	Social	0.005, 0.013, {0.001, 0.003, 0.005}

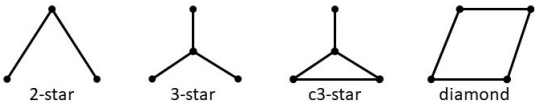

Fig. 5: Patterns used in our experiments

VI. Experimental Results

We run experiments to demonstrate the effectiveness and efficiency of our methods. Our C++ code [74] is executed on one core of a 512GB, 2.4GHz Xeon server running Ubuntu.

A. Experimental Setup

Real-world datasets (Table II). **(1)** Karate Club [75] is a social network of a university karate club. Nodes are club members and edges are interactions. **(2)** Intel Lab [76] is a collection of sensor communication data with 54 sensors deployed in the Intel Berkeley Research Lab between February 28 and April 5, 2004. **(3)** LastFM [77] is a musical social network where users listen to music. An edge between two users exists if they communicate at least once. **(4)** Homo Sapiens [78] is a protein interaction network. Nodes are proteins and edges are interactions between proteins. **(5)** Biomine [79] is constructed by integrating cross-references from biological databases. Nodes represent biological concepts such as genes, proteins etc., and edges denote real-world phenomena between two nodes, e.g., a gene "code" for a protein. **(6)** Twitter [80] is a widely used social network where nodes are users and edges are retweets. **(7)** Friendster [81] is a social network with nodes (users) and edges (friendships).

Edge probability models. We adopt widely used models for generating edge probabilities. In **(1)** Karate Club, **(6)** Twitter, and **(7)** Friendster, we assign the probability of an edge as $1-e^{-\frac{t}{\mu}}$, which is an exponential cdf of mean μ to the number t of communications between the two users. We set $\mu = 20$ [82]. In **(2)** Intel Lab, a (real) edge probability denotes the fraction of messages from the sender that successfully reached the receiver [76], [30]. In **(3)** LastFM, the probability of any edge is the reciprocal of the larger of the out-degrees of its source and target nodes [82]. In **(4)** Homo Sapiens, an edge probability is the confidence on the existence of the corresponding interaction, based on real biological experiments [78]. In **(5)** Biomine [79], an edge probability quantifies the existence of a phenomenon between the two endpoints, which combines relevance, informativeness, and confidence [29], [35], [36].

TABLE III: Densest subgraph containment probabilities of the NDS, the expected densest subgraph (EDS), the innermost η-core and γ-truss ($\eta = \gamma = 0.1$); Expected densities of the NDS and EDS

Dataset	Containment Probability				Expected Density	
	NDS	EDS	Core	Truss	NDS	EDS
Homo Sapiens	**1**	0.05	**1**	**1**	54	**54.62**
Biomine	**1**	0.01	0.99	0	46.45	**48.02**
Twitter	**1**	0	0.95	0	37.65	**38.64**

TABLE IV: Densest subgraph probabilities of the MPDS, the expected densest subgraph (EDS), the innermost η-core and γ-truss ($\eta = \gamma = 0.1$); Expected densities of the MPDS and EDS

Dataset	Densest Subgraph Probability				Expected Density	
	MPDS	EDS	Core	Truss	MPDS	EDS
Karate Club	**0.012**	0	0	0	0.703	**0.75**
Intel Lab	**0.078**	0.01	0.01	0	3.246	**3.25**
LastFM	**0.075**	0	0.04	0.02	0.667	**0.86**

TABLE V: Probabilistic density of our proposed subgraphs (MPDS for the two smaller datasets and NDS for the two larger ones) and of existing dense subgraphs in uncertain graphs

Dataset	Probabilistic Density			
	MPDS/NDS	EDS	Core	Truss
Karate Club	**0.281**	0.095	0.073	0.134
LastFM	**0.333**	0.007	0.008	0.013
Biomine	**0.546**	0.191	0.212	0.538
Twitter	**0.789**	0.042	0.121	0.781

TABLE VI: Probabilistic clustering coefficient of our proposed subgraphs (MPDS for the two smaller datasets and NDS for the two larger ones) and of existing dense subgraphs in uncertain graphs

Dataset	Probabilistic Clustering Coefficient			
	MPDS/NDS	EDS	Core	Truss
Karate Club	**0.284**	0.150	0.094	0.158
LastFM	**0.333**	0.002	0.022	0.257
Biomine	**0.546**	0.203	0.217	0.539
Twitter	**0.775**	0.142	0.253	0.768

Methods compared. We compare our MPDS and NDS algorithms with those for computing the expected densest subgraph [42], (k, η)-core [35], and (k, γ)-truss [36] (§ VI-B). As discussed in § II-C, we show the results for MPDS on the three smaller datasets and NDS on the four larger ones.

Parameters. • h **for Clique-MPDS/NDS**: We vary $h \in \{3, 4, 5\}$ [20]. $h = 2$ denotes an edge. • ψ **for Pattern-MPDS/NDS**: We vary $\psi \in \{$2-star, 3-star, c3-star, diamond$\}$ [5] (Figure 5). • **Top-k MPDSs**: We vary $k \in \{1, 5, 10\}$, with default value 1. • **Top-k NDSs**: We vary $k \in \{1, 5, 10, 50, 100\}$. • **Min. size threshold** l_m: We vary $l_m \in [1, 750]$. Beyond that range, no NDS is returned for our datasets. • **# Sampled worlds** θ: We vary $\theta \in \{2^0 \times 10, 2^1 \times 10, \ldots, 2^8 \times 10\}$. The default value is chosen as in § VI-F.

B. Comparison with Expected Density, Core, and Truss Decompositions in Uncertain Graphs

We compare our MPDS/ NDS with some existing or close notions of densest subgraphs in uncertain graphs: expected densest subgraph (EDS) [42], innermost η-core [35], and innermost γ-truss [36]. As shown in Table III, the containment probability of the η-core is comparable to (yet not greater than) that of the NDS for all datasets, in contrast to the EDS and the γ-truss. This makes sense for the following reason. The innermost η-core is likely to be an innermost core (and hence a reasonably dense subgraph [5]) of a possible world of the input graph. However, the same cannot be said about the other subgraphs. Table III demonstrates that our solution produces the most optimal node set with the highest densest subgraph containment probability compared to the other approaches. In addition, for each of our smaller datasets, we compare the densest subgraph probability of the MPDS with those of the EDS, innermost η-core and innermost γ-truss. As shown in Table IV, the MPDS outperforms the other subgraphs.

Since the EDS performs very poorly for all datasets, for fairness, we compare the expected densities of the EDS and our NDS/MPDS. Tables III and IV show that our solutions produce subgraphs with expected densities comparable to the optimal values, thereby showing that our returned subgraphs are good even with respect to expected density.

We also consider two *external* evaluation metrics: • *Probabilistic Density* $PD(U)$ [36] for capturing the cohesiveness of a probabilistic subgraph U, which is defined as the weighted sum of existing edges divided by the maximum number of possible edges this subgraph can have (Equation 16); and • *Probabilistic Clustering Coefficient* $PCC(U)$ [83] for measuring how well the nodes in a probabilistic subgraph U cluster together, which is computed as three times the weighted sum of all possible triangles divided by the weighted sum of all neighboring edge pairs. The weights are existence probabilities of edges/triangles/neighboring edge pairs, assuming independence among edges (Equation 17). V_U, E_U, and Δ_U denote the set of nodes, edges, and triangles in U, respectively.

$$PD(U) = \frac{\sum_{e \in E_U} p(e)}{\frac{1}{2}|V_U|(|V_U| - 1)} \tag{16}$$

$$PCC(U) = \frac{3 \sum_{\triangle_{uvw} \in \Delta_U} p(u,v)p(u,w)p(v,w)}{\sum_{(u,v),(u,w) \in E_U, v \neq w} p(u,v)p(u,w)} \tag{17}$$

Tables V-VI demonstrate that our NDS/MPDS significantly outperforms other dense subgraph notions based on both probabilistic density and probabilistic clustering coefficient, implying that the NDS/MPDS is much more cohesive, i.e., most of the possible edges induced by the NDS/MPDS node set tend to exist, and the nodes in the NDS/MPDS cluster together. Only the innermost truss achieves slightly lower results on the two larger datasets.

TABLE VII: Purity (§ VI-C) of the node sets in the top-k MPDSs and in the existing notions of dense subgraphs over Karate Club uncertain graph. There are only two cores and two trusses in this graph; thus the entries for $k > 2$ are empty for those subgraphs.

Top-k	Purity			
	MPDS	EDS	Core	Truss
1	**1**	0.6	0.5	0.538
2	**1**	0.6	0.515	0.536
5	**1**	0.749	-	-
10	**1**	0.699	-	-

C. Case Studies: Karate Club Network

Densest subgraphs in social networks can correspond to communities [6], filter bubbles and echo chambers [7], [8]. Table VI already shows that the MPDS of the Karate Club dataset has a much higher probabilistic clustering coefficient than the other existing dense subgraph notions. We show that the MPDS also represents a more meaningful and concise community (of club members) than the other subgraphs. All four subgraphs are shown in Figure 6. Notice that the MPDS only contains nodes from one single ground-truth community

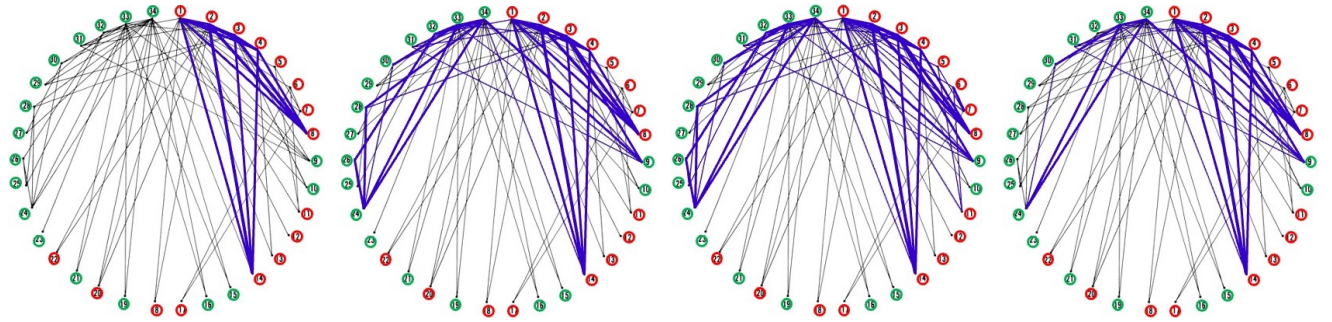

(a) MPDS (b) Expected Densest Subgraph (c) Innermost core (d) Innermost truss

Fig. 6: Case studies to compare with existing dense subgraphs in uncertain graphs on the Karate Club dataset. The relevant subgraphs are in blue, while the colour of a node denotes its ground-truth community [75]. The thickness of each edge is proportional to its probability.

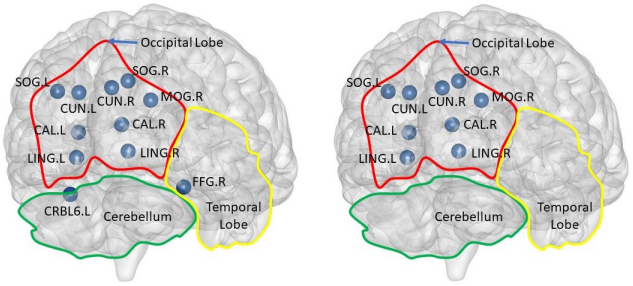

(a) Typically developed (b) ASD-affected

Fig. 7: Node sets of 3-clique MPDSs in brain networks. The colored boundaries denote the cerebellum, occipital, and temporal lobes.

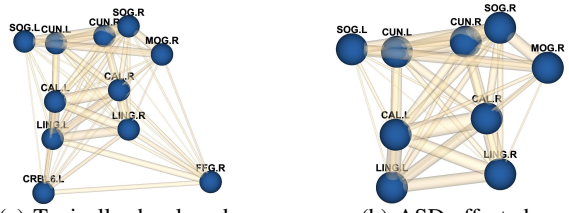

(a) Typically developed (b) ASD-affected

Fig. 8: 3-clique MPDSs in brain networks. The thickness of each edge is proportional to its probability.

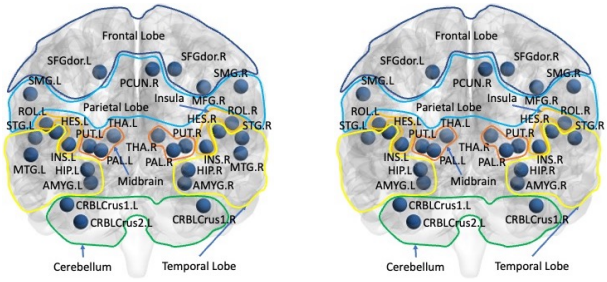

(a) Typically developed (b) ASD-affected

Fig. 9: Node sets of 3-clique EDSs in brain networks. The colored boundaries denote various brain regions as shown.

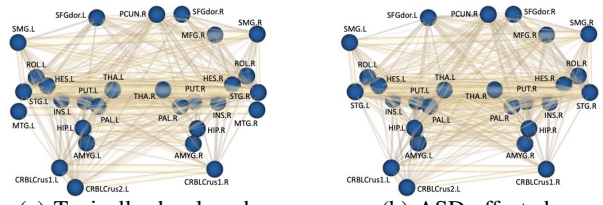

(a) Typically developed (b) ASD-affected

Fig. 10: 3-clique EDSs in brain networks. The thickness of each edge is proportional to its probability.

[75] and has edges with higher probabilities, in contrast to all the other subgraphs which contain nodes from both communities and have many low-probability edges. Moreover, in Table VII, we report the average purity (i.e., the highest fraction of nodes from the same ground-truth community [75] in a node set) of the top-k (up to $k = 10$) subgraphs returned by each notion, and observe that MPDSs always achieve 100% purity. Thus, users can retrieve the top-k MPDSs to identify high-quality communities. This case study highlights the importance of computing MPDSs despite other notions of dense subgraphs in uncertain graphs.

D. Case Studies: Brain Networks

A brain network can be defined as an uncertain graph where nodes are brain regions of interest (ROIs), an edge indicates co-activation between two ROIs, and an edge probability indicates the strength of the co-activation signal. Dense subgraphs in brain networks can represent brain regions responding together to stimuli [9] or related to diseases [10].

The dataset we use [84] contains data of 52 *Typically Developed* (TD) children and 49 children suffering from *Autism Spectrum Disorder* (ASD). Each subject is represented as a graph over 116 nodes (ROIs). $\mathcal{G}_{ASD}$ and $\mathcal{G}_{TD}$ are uncertain graphs, defined over the same set of nodes as the original ones, while the probability of each edge is the average of those of the same edge across all graphs in the ASD and TD groups.

Using BrainNet Viewer [85], we show the 3-clique MPDSs for both $\mathcal{G}_{TD}$ and $\mathcal{G}_{ASD}$ in Figures 7 and 8. The MPDS in $\mathcal{G}_{ASD}$ lies entirely in the occipital lobe, in contrast to that in $\mathcal{G}_{TD}$, which also contains one node in the temporal lobe and one in the cerebellum. Besides, the MPDS in $\mathcal{G}_{ASD}$ is more symmetrical than that in $\mathcal{G}_{TD}$, since the former has only one node (MOG.R) without its counterpart in the other hemisphere, while the latter has two more such nodes (CRBL6.L and FFG.R). This is consistent with the results of different works in neuroscience indicating that, in contrast to typically developed brains, those affected by ASD are characterized by under-connectivity between distant brain regions and over-connectivity between closer ones [86], [87], and that the hemispheres of ASD-affected brains are more symmetrical than those of typically developed ones [88]. Our consistent findings underline the importance of finding MPDSs in uncertain brain networks that can differentiate healthy and autistic brains.

We now show that the expected (3-clique) densest subgraph (EDS) cannot characterize and distinguish autistic brains,

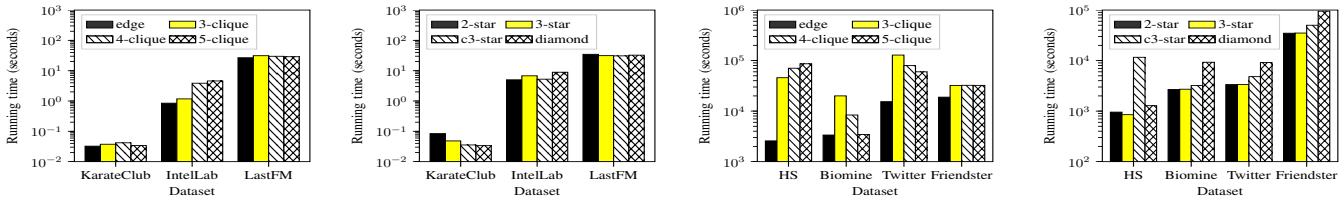

(a) Edge and Clique-MPDS (b) Pattern-MPDS (c) Edge and Clique-NDS (d) Heuristic Pattern-NDS

Fig. 11: Running times of our proposed methods; MPDS for the smaller datasets and NDS for the larger ones; HS denotes HomoSapiens

unlike our proposed MPDS. The EDS notion was defined for edge density [42]; however, we show that it can be extended to clique and pattern densities (in [50]). Figures 9 and 10 present 3-clique EDSs in both $\mathcal{G}_{TD}$ and $\mathcal{G}_{ASD}$. Both of them span as many as 9 brain regions and are similar (w.r.t. symmetry) since both only have the same 3 nodes (PCUN.R, MFG.R and CRBLCrus2.L) without their counterparts in the other hemispheres. These contradict the characteristics of autistic brains in the biological literature [86], [87], [88] and fail to distinguish them from normal ones. This is consistent with our observation in Example 1 that EDSs tend to be very large and span several unimportant nodes, and hence can be less meaningful in real-world applications. Our MPDS is more powerful than the existing EDS in analyzing autistic brains. We also show in [50] that the innermost core and the innermost truss cannot characterize and distinguish autistic brains.

E. Efficiency

We report the running times of our methods in Figure 11. As shown in Figures 11(a) and 11(c), the running times for edge density are smaller than those for clique density. This is because the flow networks involved in computing edge densest subgraphs are much smaller; they only contain nodes for each node in the sampled possible worlds (§ III-A), in contrast to those for h-clique densest subgraphs which also contain nodes for each $(h-1)$-clique contained in h-cliques in the sampled possible worlds (§ III-B). However, there is no clear winner among 3-clique, 4-clique, and 5-clique. This is because, even if larger cliques take a longer time to enumerate, smaller cliques can be more in number, thereby increasing the size of the flow network and hence the running time. Similar arguments can be made for the four patterns (Figures 11(b) and 11(d)).

F. Parameter Sensitivity

Varying θ. We study the effects of the variation of θ in Figure 12. As in § VI-E, although we show the results for only two datasets, the other datasets exhibit similar trends. For MPDS on the Intel Lab dataset (Figure 12(a)), increasing θ steadily increases the similarity of the returned node sets to those for the previous value of θ till a certain point ($\theta = 160$), after which it converges, while the running time keeps increasing. Similar effects can be observed at $\theta = 640$ for NDS on the Biomine dataset (Figure 12(b)). We choose such values of θ as default for the respective datasets in our experiments.

Varying k for top-k NDSs. Figure 13(a) shows that increasing the value of k results in the reduction of the average estimated densest subgraph containment probability. This shows that increasing the value of k too much results in the returned node sets being of lower quality.

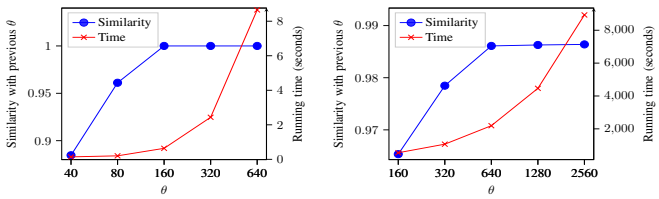

(a) MPDS; Intel Lab (b) NDS; Biomine

Fig. 12: Variation, w.r.t. θ, of the running time and the similarity of the returned node sets to those for the previous value of θ

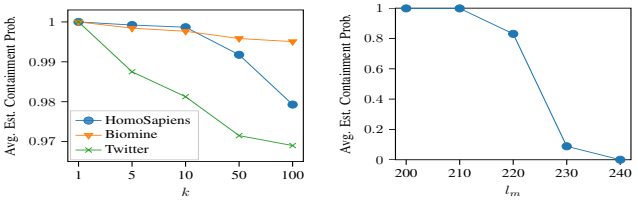

(a) Varying k (b) Varying l_m; Homo Sapiens

Fig. 13: Variation of the average estimated densest subgraph containment probability with k and l_m for NDS queries

Varying l_m. Figure 13(b) shows the variation of the average estimated densest subgraph containment probability with increasing l_m. Till a certain value of l_m, the probability remains constant; since the returned node sets should be closed, our algorithm avoids reporting too small node sets even for smaller values of l_m. After that, the probability keeps decreasing with l_m till a certain value beyond which it remains 0 as there is no larger closed node set. This helps in choosing a feasible upper bound on l_m for a specific dataset.

VII. Conclusions

We studied the novel problem of finding the Most Probable Densest Subgraph (MPDS) in an uncertain graph, according to edge, clique, and pattern densities. We proved that computing the densest subgraph probability for any given node set is $\#\mathbf{P}$-hard. We proposed a solution which returns the most frequent densest subgraphs from some sampled worlds, with theoretical accuracy guarantees. As building blocks, we designed novel algorithms to compute all clique- and pattern-densest subgraphs in a deterministic graph. We then extended our algorithm to compute the Nucleus Densest Subgraphs (NDS) via reduction to closed frequent itemset mining. Our experiments on large real-world graphs showed that our methods are efficient. Our case studies showcased the usefulness of MPDS in differentiating autistic brains from healthy ones and in detecting useful communities in social networks.

REFERENCES

[1] A. V. Goldberg, *Finding a Maximum Density Subgraph*. University of California Berkeley, 1984.

[2] M. Charikar, "Greedy approximation algorithms for finding dense components in a graph," in *International Workshop on Approximation Algorithms for Combinatorial Optimization*. Berlin, Heidelberg: Springer, 2000, pp. 84–95.

[3] C. Tsourakakis, F. Bonchi, A. Gionis, F. Gullo, and M. Tsiarli, "Denser than the densest subgraph: Extracting optimal quasi-cliques with quality guarantees," in *Proceedings of the 19th ACM SIGKDD International Conference on Knowledge Discovery and Data Mining*, 2013, p. 104–112.

[4] A. Gionis and C. E. Tsourakakis, "Dense subgraph discovery," in *Proceedings of the 21th ACM SIGKDD International Conference on Knowledge Discovery and Data Mining*, 2015, p. 2313–2314.

[5] Y. Fang, K. Yu, R. Cheng, L. V. Lakshmanan, and X. Lin, "Efficient algorithms for densest subgraph discovery," *Proceedings of the VLDB Endowment*, vol. 12, no. 11, p. 1719–1732, 2019.

[6] Y. Dourisboure, F. Geraci, and M. Pellegrini, "Extraction and classification of dense implicit communities in the web graph," *ACM Transactions on the Web*, vol. 3, no. 2, pp. 1–36, 2009.

[7] K. Asatani, H. Yamano, T. Sakaki, and I. Sakata, "Dense and influential core promotion of daily viral information spread in political echo chambers," *Scientific reports*, vol. 11, no. 1, pp. 1–10, 2021.

[8] L. V. Lakshmanan, "On a quest for combating filter bubbles and misinformation," in *Proceedings of the 2022 ACM SIGMOD International Conference on Management of Data*, 2022, p. 2.

[9] R. Legenstein, W. Maass, C. H. Papadimitriou, and S. S. Vempala, "Long term memory and the densest k-subgraph problem," in *9th Innovations in Theoretical Computer Science Conference (ITCS 2018)*, ser. Leibniz International Proceedings in Informatics (LIPIcs), vol. 94. Dagstuhl, Germany: Schloss Dagstuhl–Leibniz-Zentrum fuer Informatik, 2018, pp. 57:1–57:15.

[10] Q. Wu, X. Huang, A. J. Culbreth, J. A. Waltz, L. E. Hong, and S. Chen, "Extracting brain disease-related connectome subgraphs by adaptive dense subgraph discovery," *Biometrics*, 2021.

[11] X. Du, R. Jin, L. Ding, V. E. Lee, and J. H. Thornton, "Migration motif: A spatial-temporal pattern mining approach for financial markets," in *Proceedings of the 15th ACM SIGKDD International Conference on Knowledge Discovery and Data Mining*, 2009, p. 1135–1144.

[12] G. Buehrer and K. Chellapilla, "A scalable pattern mining approach to web graph compression with communities," in *Proceedings of the 2008 International Conference on Web Search and Data Mining*, 2008, p. 95–106.

[13] Y. Zhang and S. Parthasarathy, "Extracting analyzing and visualizing triangle k-core motifs within networks," in *IEEE 28th international conference on data engineering*, 2012, pp. 1049–1060.

[14] F. Zhao and A. K. H. Tung, "Large scale cohesive subgraphs discovery for social network visual analysis," *Proceedings of the VLDB Endowment*, vol. 6, no. 2, p. 85–96, 2012.

[15] E. Cohen, E. Halperin, H. Kaplan, and U. Zwick, "Reachability and distance queries via 2-hop labels," in *Proceedings of the 13th Annual ACM-SIAM Symposium on Discrete Algorithms*. USA: Society for Industrial and Applied Mathematics, 2002, p. 937–946.

[16] R. Jin, Y. Xiang, N. Ruan, and D. Fuhry, "3-hop: A high-compression indexing scheme for reachability query," in *Proceedings of the 2009 ACM SIGMOD International Conference on Management of Data*, 2009, p. 813–826.

[17] A. Gionis, F. Junqueira, V. Leroy, M. Serafini, and I. Weber, "Piggybacking on social networks," *Proceedings of the VLDB Endowment*, vol. 6, no. 6, p. 409–420, 2013.

[18] A. Faragó and Z. R. Mojaveri, "In search of the densest subgraph," *Algorithms*, vol. 12, no. 8, p. 157, 2019.

[19] C. E. Tsourakakis, "The k-clique densest subgraph problem," in *Proceedings of the 24th International Conference on World Wide Web*. Republic and Canton of Geneva, CHE: International World Wide Web Conferences Steering Committee, 2015, p. 1122–1132.

[20] M. Mitzenmacher, J. Pachocki, R. Peng, C. E. Tsourakakis, and S. C. Xu, "Scalable large near-clique detection in large-scale networks via sampling," in *Proceedings of the 21st ACM SIGKDD International Conference on Knowledge Discovery and Data Mining*, 2015, p. 815–824.

[21] H. Yanagisawa and S. Hara, "Discounted average degree density metric and new algorithms for the densest subgraph problem," *Networks*, vol. 71, no. 1, pp. 3–15, 2018.

[22] C. C. Aggarwal, *Managing and Mining Uncertain Data*, ser. Advances in Database Systems. Boston, MA, USA: Springer, 2009, vol. 35.

[23] E. Adar and C. Ré, "Managing uncertainty in social networks," *IEEE Data Engineering Bulletin*, vol. 30, no. 2, pp. 15–22, 2007.

[24] D. Liben-Nowell and J. Kleinberg, "The link prediction problem for social networks," in *Proceedings of the 12th International Conference on Information and Knowledge Management*, 2003, p. 556–559.

[25] P. Boldi, F. Bonchi, A. Gionis, and T. Tassa, "Injecting uncertainty in graphs for identity obfuscation," *Proceedings of the VLDB Endowment*, vol. 5, no. 11, p. 1376–1387, 2012.

[26] A. Khan, Y. Ye, and L. Chen, *On Uncertain Graphs*, ser. Synthesis Lectures on Data Management. Morgan & Claypool Publishers, 2018, vol. 10.

[27] V. Kassiano, A. Gounaris, A. N. Papadopoulos, and K. Tsichlas, "Mining uncertain graphs: An overview," in *International Workshop of Algorithmic Aspects of Cloud Computing*. Cham: Springer, 2016, pp. 87–116.

[28] A. Khan and L. Chen, "On uncertain graphs modeling and queries," *Proceedings of the VLDB Endowment*, vol. 8, no. 12, p. 2042–2043, 2015.

[29] M. Potamias, F. Bonchi, A. Gionis, and G. Kollios, "k-nearest neighbors in uncertain graphs," *Proceedings of the VLDB Endowment*, vol. 3, no. 1–2, p. 997–1008, 2010.

[30] A. Saha, R. Brokkelkamp, Y. Velaj, A. Khan, and F. Bonchi, "Shortest paths and centrality in uncertain networks," *Proceedings of the VLDB Endowment*, vol. 14, no. 7, p. 1188–1201, 2021.

[31] A. P. Mukherjee, P. Xu, and S. Tirthapura, "Enumeration of maximal cliques from an uncertain graph," *IEEE Transactions on Knowledge and Data Engineering*, vol. 29, no. 3, pp. 543–555, 2016.

[32] Z. Zou, J. Li, H. Gao, and S. Zhang, "Finding top-k maximal cliques in an uncertain graph," in *IEEE 26th International Conference on Data Engineering*, 2010, pp. 649–652.

[33] R.-H. Li, Q. Dai, G. Wang, Z. Ming, L. Qin, and J. X. Yu, "Improved algorithms for maximal clique search in uncertain networks," in *IEEE 35th International Conference on Data Engineering*, 2019, pp. 1178–1189.

[34] Q. Dai, R.-H. Li, M. Liao, H. Chen, and G. Wang, "Fast maximal clique enumeration on uncertain graphs: A pivot-based approach," in *Proceedings of the 2022 ACM SIGMOD International Conference on Management of Data*, 2022, p. 2034–2047.

[35] F. Bonchi, F. Gullo, A. Kaltenbrunner, and Y. Volkovich, "Core decomposition of uncertain graphs," in *Proceedings of the 20th ACM SIGKDD International Conference on Knowledge Discovery and Data Mining*, 2014, p. 1316–1325.

[36] X. Huang, W. Lu, and L. V. Lakshmanan, "Truss decomposition of probabilistic graphs: Semantics and algorithms," in *Proceedings of the 2016 ACM SIGMOD International Conference on Management of Data*, 2016, p. 77–90.

[37] L. Liu, R. Jin, C. C. Aggarwal, and Y. Shen, "Reliable clustering on uncertain graphs," in *IEEE International Conference on Data Mining*, 2012, pp. 459–468.

[38] K. Han, F. Gui, X. Xiao, J. Tang, Y. He, Z. Cao, and H. Huang, "Efficient and effective algorithms for clustering uncertain graphs," *Proceedings of the VLDB Endowment*, vol. 12, no. 6, p. 667–680, 2019.

[39] M. Ceccarello, C. Fantozzi, A. Pietracaprina, G. Pucci, and F. Vandin, "Clustering uncertain graphs," *Proceedings of the VLDB Endowment*, vol. 11, no. 4, pp. 472–484, 2017.

[40] R. Jin, L. Liu, and C. C. Aggarwal, "Discovering highly reliable subgraphs in uncertain graphs," in *Proceedings of the 17th ACM International Conference on Knowledge Discovery and Data Mining*. ACM, 2011, pp. 992–1000.

[41] C. Ma, R. Cheng, L. V. Lakshmanan, T. Grubenmann, Y. Fang, and X. Li, "Linc: A motif counting algorithm for uncertain graphs," *Proceedings of the VLDB Endowment*, vol. 13, no. 2, p. 155–168, 2019.

[42] Z. Zou, "Polynomial-time algorithm for finding densest subgraphs in uncertain graphs," in *Proceedings of the 11th Workshop on Mining and Learning with Graphs*, 2013.

[43] L. Chang and M. Qiao, "Deconstruct densest subgraphs," in *Proceedings of the 29th International Conference on World Wide Web*, 2020, p. 2747–2753.

[44] J. Wang, J. Han, Y. Lu, and P. Tzvetkov, "Tfp: an efficient algorithm for mining top-k frequent closed itemsets," *IEEE Transactions on Knowledge and Data Engineering*, vol. 17, no. 5, pp. 652–663, 2005.

[45] L. G. Valiant, "The complexity of enumeration and reliability problems," *SIAM Journal on Computing*, vol. 8, no. 3, pp. 410–421, 1979.

[46] M. O. Ball, "Computational complexity of network reliability analysis: An overview," *IEEE Transactions on Reliability*, vol. 35, no. 3, pp. 230–239, 1986.

[47] A. Khan, F. Bonchi, F. Gullo, and A. Nufer, "Conditional reliability in uncertain graphs," *IEEE Transactions on Knowledge and Data Engineering*, vol. 30, no. 11, pp. 2078–2092, 2018.

[48] J. Chen and Y. Saad, "Dense subgraph extraction with application to community detection," *TKDE*, vol. 24, no. 7, pp. 1216–1230, 2012.

[49] H. Yin, A. R. Benson, J. Leskovec, and D. F. Gleich, "Local higher-order graph clustering," in *Proceedings of the 23rd ACM SIGKDD International Conference on Knowledge Discovery and Data Mining*. New York, NY, USA: ACM, 2017, pp. 555–564.

[50] A. Saha, X. Ke, A. Khan, and C. Long, "Most probable densest subgraphs," 2022. [Online]. Available: https://arxiv.org/abs/2212.08820

[51] V. Batagelj and M. Zaversnik, "An o(m) algorithm for cores decomposition of networks," *CoRR*, vol. cs.DS/0310049, 2003.

[52] Y. Li, J. Fan, D. Zhang, and K.-L. Tan, "Discovering your selling points: Personalized social influential tags exploration," in *Proceedings of the 2017 ACM SIGMOD International Conference on Management of Data*, 2017, p. 619–634.

[53] R.-H. Li, J. X. Yu, R. Mao, and T. Jin, "Recursive stratified sampling: A new framework for query evaluation on uncertain graphs," *IEEE Transactions on Knowledge and Data Engineering*, vol. 28, no. 2, pp. 468–482, 2016.

[54] M. Danisch, O. D. Balalau, and M. Sozio, "Listing k-cliques in sparse real-world graphs," in *Proceedings of the 2018 World Wide Web Conference*. Republic and Canton of Geneva, CHE: International World Wide Web Conferences Steering Committee, 2018, p. 589–598.

[55] B. Sun, M. Danisch, T.-H. H. Chan, and M. Sozio, "Kclist++: A simple algorithm for finding k-clique densest subgraphs in large graphs," *Proceedings of the VLDB Endowment*, vol. 13, no. 10, p. 1628–1640, 2020.

[56] M. Qiao, H. Zhang, and H. Cheng, "Subgraph matching: On compression and computation," *Proceedings of the VLDB Endowment*, vol. 11, no. 2, p. 176–188, 2017.

[57] O. D. Balalau, F. Bonchi, T.-H. H. Chan, F. Gullo, and M. Sozio, "Finding subgraphs with maximum total density and limited overlap," in *Proceedings of the Eighth ACM International Conference on Web Search and Data Mining*, 2015, p. 379–388.

[58] B. Bahmani, R. Kumar, and S. Vassilvitskii, "Densest subgraph in streaming and mapreduce," *Proc. VLDB Endow.*, vol. 5, no. 5, p. 454–465, jan 2012.

[59] S. Sawlani and J. Wang, "Near-optimal fully dynamic densest subgraph," in *Proceedings of the 52nd Annual ACM SIGACT Symposium on Theory of Computing*, ser. STOC 2020. New York, NY, USA: Association for Computing Machinery, 2020, p. 181–193.

[60] R. Andersen and K. Chellapilla, "Finding dense subgraphs with size bounds," in *Algorithms and Models for the Web-Graph*, K. Avrachenkov, D. Donato, and N. Litvak, Eds. Berlin, Heidelberg: Springer Berlin Heidelberg, 2009, pp. 25–37.

[61] M. A. U. Nasir, A. Gionis, G. D. F. Morales, and S. Girdzijauskas, "Fully dynamic algorithm for top-k densest subgraphs," in *Proceedings of the 2017 ACM on Conference on Information and Knowledge Management*, ser. CIKM '17. New York, NY, USA: Association for Computing Machinery, 2017, p. 1817–1826.

[62] L. Qin, R.-H. Li, L. Chang, and C. Zhang, "Locally densest subgraph discovery," in *Proceedings of the 21th ACM SIGKDD International Conference on Knowledge Discovery and Data Mining*, ser. KDD '15. New York, NY, USA: Association for Computing Machinery, 2015, p. 965–974.

[63] M. Danisch, T.-H. H. Chan, and M. Sozio, "Large scale density-friendly graph decomposition via convex programming," in *Proceedings of the 26th International Conference on World Wide Web*, ser. WWW '17. Republic and Canton of Geneva, CHE: International World Wide Web Conferences Steering Committee, 2017, p. 233–242.

[64] N. Tatti, "Density-friendly graph decomposition," *ACM Trans. Knowl. Discov. Data*, vol. 13, no. 5, sep 2019.

[65] C. Ma, Y. Fang, R. Cheng, L. V. Lakshmanan, W. Zhang, and X. Lin, "Efficient algorithms for densest subgraph discovery on large directed graphs," in *Proceedings of the 2020 ACM SIGMOD International Conference on Management of Data*, ser. SIGMOD '20. New York, NY, USA: Association for Computing Machinery, 2020, p. 1051–1066.

[66] B. Hooi, H. A. Song, A. Beutel, N. Shah, K. Shin, and C. Faloutsos, "Fraudar: Bounding graph fraud in the face of camouflage," in *Proceedings of the 22nd ACM SIGKDD International Conference on Knowledge Discovery and Data Mining*, ser. KDD '16. New York, NY, USA: Association for Computing Machinery, 2016, p. 895–904.

[67] E. Galimberti, F. Bonchi, F. Gullo, and T. Lanciano, "Core decomposition in multilayer networks: Theory, algorithms, and applications," *ACM Trans. Knowl. Discov. Data*, vol. 14, no. 1, jan 2020.

[68] Y. Fang, W. Luo, and C. Ma, "Densest subgraph discovery on large graphs: Applications, challenges, and techniques," *Proc. VLDB Endow.*, vol. 15, no. 12, pp. 3766–3769, 2022.

[69] F. Esfahani, J. Wu, V. Srinivasan, A. Thomo, and K. Wu, "Fast truss decomposition in large-scale probabilistic graphs," in *22nd International Conference on Extending Database Technology*, 2019, pp. 722–725.

[70] D. Seux, F. Malliaros, A. Papadopoulos, and M. Vazirgiannis, "Core decomposition of uncertain graphs using representative instances," in *6th International Conference on Complex Networks and Their Applications*, 2017.

[71] Q. Dai, R. Li, G. Wang, R. Mao, Z. Zhang, and Y. Yuan, "Core decomposition on uncertain graphs revisited," *IEEE Transactions on Knowledge and Data Engineering*, 2021.

[72] Z. Sun, X. Huang, J. Xu, and F. Bonchi, "Efficient probabilistic truss indexing on uncertain graphs," in *The Web Conference*. ACM / IW3C2, 2021, pp. 354–366.

[73] Z. Zou and R. Zhu, "Truss decomposition of uncertain graphs," *Knowledge and Information Systems*, vol. 50, no. 1, pp. 197–230, 2017.

[74] A. Saha, X. Ke, A. Khan, and C. Long, "Most probable densest subgraphs: Code and data," 2022. [Online]. Available: https://github.com/ArkaSaha/MPDS

[75] W. W. Zachary, "An information flow model for conflict and fission in small groups," *Journal of anthropological research*, vol. 33, no. 4, pp. 452–473, 1977.

[76] S. Madden, "Intel lab data," 2004. [Online]. Available: http://db.csail.mit.edu/labdata/labdata.html

[77] "Lastfm api," 2002. [Online]. Available: https://www.last.fm

[78] D. Szklarczyk, A. L. Gable, K. C. Nastou, D. Lyon, R. Kirsch, S. Pyysalo, N. T. Doncheva, M. Legeay, T. Fang, P. Bork *et al.*, "The string database in 2021: Customizable protein–protein networks, and functional characterization of user-uploaded gene/measurement sets," *Nucleic Acids Research*, vol. 49, no. D1, pp. D605–D612, 2021.

[79] L. Eronen and H. Toivonen, "Biomine: Predicting links between biological entities using network models of heterogeneous databases," *BMC Bioinformatics*, vol. 13, no. 1, 2012.

[80] J. Leskovec and A. Krevl, "SNAP Datasets: Stanford large network dataset collection," http://snap.stanford.edu/data, 2014.

[81] J. Yang and J. Leskovec, "Defining and evaluating network communities based on ground-truth," *Knowledge and Information Systems*, vol. 42, pp. 181–213, 2015.

[82] X. Ke, A. Khan, M. Al Hasan, and R. Rezvansangsari, "Reliability maximization in uncertain graphs," *IEEE Transactions on Knowledge and Data Engineering*, vol. 34, no. 2, pp. 894–913, 2022.

[83] J. J. Pfeiffer III and J. Neville, "Methods to determine node centrality and clustering in graphs with uncertain structure," in *Fifth International AAAI Conference on Weblogs and Social Media*, 2011.

[84] C. Craddock, Y. Benhajali, C. Chu, F. Chouinard, A. Evans, A. Jakab, B. S. Khundrakpam, J. D. Lewis, Q. Li, M. Milham, C. Yan, and P. Bellec, "The neuro bureau preprocessing initiative: Open sharing of preprocessed neuroimaging data and derivatives," *Frontiers in Neuroinformatics*, 2013.

[85] M. Xia, J. Wang, and Y. He, "Brainnet viewer: a network visualization tool for human brain connectomics," *PloS one*, vol. 8, no. 7, p. e68910, 2013.

[86] A. Di Martino, C. Kelly, R. Grzadzinski, X.-N. Zuo, M. Mennes, M. Mairena, C. Lord, F. Castellanos, and M. Milham, "Aberrant striatal functional connectivity in children with autism," *Biological Psychiatry*, vol. 69, no. 9, pp. 847–56, 12 2010.

[87] S. Noonan, F. Haist, and R.-A. Müller, "Aberrant functional connectivity in autism: Evidence from low-frequency bold signal fluctuations," *Brain Research*, vol. 1262, pp. 48–63, 02 2009.

[88] M. Postema, D. Van Rooij, E. Anagnostou, C. Arango, G. Auzias, M. Behrmann, G. Busatto, S. Calderoni, R. Calvo, E. Daly, C. Deruelle, A. Di Martino, I. Dinstein, F. Duran, S. Durston, C. Ecker, S. Ehrlich, D. Fair, J. Fedor, and C. Francks, "Altered structural brain asymmetry in autism spectrum disorder in a study of 54 datasets," *Nature Communications*, vol. 10, 12 2019.